https://doi.org/10.5194/egusphere-2024-579
Preprint. Discussion started: 25 April 2024
© Author(s) 2024. CC BY 4.0 License.

A new dunetracking tool to support input parameter selection and uncertainty analyses using a Monte Carlo approach

Julius Reich[1], Axel Winterscheid[1]

[1]Federal Institute of Hydrology, Department M3 – Fluvial Morphology, Sediment Dynamics and Management, Koblenz, 56068, Germany

Correspondence to: Julius Reich (reich@bafg.de)

Abstract. Precise and reliable information about bedforms, regarding geometry and dynamics, is relevant for many applications – like ensuring safe conditions for navigation along the waterways, parameterizing the roughness of the riverbed in numerical models, or improving bedload measurement and monitoring techniques. There are many so-called dunetracking tools to extract this information from bathymetrical data. However, most of these tools require the setting of various input parameters, which in turn influence the resulting bedform characteristics. How to set the values for these parameters and what influence they have on the calculations has not yet been comprehensively investigated. This is why we introduce a new dunetracking tool, which is able to quantify the influence of varying input parameter settings by performing a Monte Carlo Simulation. The core of the tool is a combination of the two existing applications Bedforms-ATM (Guitierrez, 2018) and RhenoBT (Frings et al., 2012), which have been extended by adding additional features. A wavelet analysis has been adapted from Bedforms-ATM while a zerocrossing procedure and a cross correlation analysis have been implemented based on RhenoBT. The combination of both tools enables a more accurate and sound procedure, as the results of the first step are required input parameters in the second step. By performing a Monte Carlo Simulation, comprehensive sensitivity analyses can be carried out and the possible range of results is revealed. At the same time, the high degree of automation allows the processing of large amounts of data. By applying the tool to a test dataset, it was found that bedform parameters react with different sensitivity to varying input parameter settings. Bedform lengths appeared to be more sensitive (uncertainties up to 50 % were identified) than bedform heights. The setting of a window size in the zerocrossing procedure (especially for the upper layer of bedforms in case secondary bedforms are present) was identified to be the most decisive input parameter. Here, however, the wavelet analysis offers orientation by providing a range of plausible input window sizes and thus allows a reduction of uncertainties. By choosing values outside this range, divergence behavior could be observed for several resulting bedform parameters. Concurrently, the time interval between two successive measurements has proven to have a significant influence on the determination of bedform dynamics. For the test dataset, the faster migrating secondary bedforms were no longer traceable for intervals longer than two hours. At the same time, they contributed to up to 90 % of the total bedload transport, highlighting the need for measurements in high temporal resolution in order to avoid a severe underestimation.

https://doi.org/10.5194/egusphere-2024-579
Preprint. Discussion started: 25 April 2024
© Author(s) 2024. CC BY 4.0 License.

1 Introduction

Bedforms are ubiquitous in rivers with sandy or gravelly beds (Carling et al., 2006; Kleinhans, 2001; Van Rijn, 1993). Their occurrence, shape and dimensions as well as their dynamics depend on hydraulic and morphological conditions. Knowing bedforms is crucial for various fields of application. For example, bedform crest heights influence the navigable depth along the waterways. This is why information about maximum bedform heights is required in order to ensure the safety and ease of navigation. From the perspective of hydraulics, bedforms increase the flow resistance at the river bed. In numerical modeling, bedform dimensions and shapes need to be parametrized and transformed into form roughness (Lefebvre and Winter, 2016; Venditti, 2013). The erosion of particles on the bedforms' upstream faces and the accumulation on their downstream faces result in a downstream movement of sediments, contributing to bedload transport (Simons et al., 1965). Therefore, bedload transport rates can be estimated based on bedform migration - so-called dunetracking (e.g. Claude et al., 2012; Leary and Buscombe, 2019; Simons et al., 1965) - representing an alternative approach to direct bedload measurements.

Over the years many dunetracking approaches were developed to derive both bedform geometries and migration rates from multibeam echosounding (MBES)-data (e.g. Gilja et al., 2016; Guitierrez et al., 2018; Van der Mark and Blom, 2007; Wang et al., 2019; Zomer et al., 2021a). Besides 2D-approaches based on the evaluation of longitudinal bed elevation profiles (BEPs), also 3D-solutions were introduced (e.g. Henning, 2013; Ogor, 2019). Most of these approaches require the setting of procedure-specific input parameters. Often, there are no theoretically sound criteria or anything like best practice for setting a specific value. For example, the zerocrossing approach is widely used to identify bedforms crests and troughs in a BEP based on the calculation of a moving average (e.g Van der Mark & Blom, 2007). This requires the setting of a window size, but there are no equations or guidelines for choosing its exact value. Therefore, the procedure is strongly influenced by the personal experience and subjective selection of the investigator. If applied by several investigators, different results will be obtained from the same procedure and for the same dataset. Despite the ubiquitous need to define the setting of these parameters, little attention has been paid on how different settings influence estimated bedform attributes. A Monte Carlo Simulation (MCS) is a suitable approach to evaluate the selection of input parameters for the calculations. By repeating the analysis several times with varying input parameters settings, the possible range of results is revealed and robust estimates can be made.

Furthermore, many existing dunetracking tools are designed to evaluate single datasets and lack the possibility of batch processing. The manual setting of input parameters and the need for repeated analyses prevent an efficient and consistent analysis when multiple data records with large spatial and temporal extent are available. This highlights the need for an objective approach that on the one hand allows the highly automated processing of large amounts of data and at the same time addresses the procedure-specific uncertainties in the setting of input parameters.

Here, we present a new dunetracking tool that builds on existing applications, combines them and adds new functionalities. The tool includes an initial wavelet analysis, a zerocrossing procedure to determine bedform geometries and two different approaches to analyze bedform dynamics. The wavelet analysis is based on Bedforms-ATM (Guitierrez, 2018). It allows initial estimates about prevailing bedform lengths in a given BEP, which is a required input parameter in the following step. Bedform

https://doi.org/10.5194/egusphere-2024-579
Preprint. Discussion started: 25 April 2024
© Author(s) 2024. CC BY 4.0 License.

geometries are determined by a zerocrossing procedure adapted from the software RhenoBT (Frings et al., 2012), which in return is based on the bedform tracking tool by Van der Mark & Blom (2007). Once bedform geometries have been determined, bedform migration and bedload transport rates are calculated based on cross-correlation analyses (analog to RhenoBT) as well as on a new method that is introduced in this study (so-called centroid analysis). Such a design enables a higher accuracy because the first step provides mathematically sound criteria for the initial setting of the input parameters (window sizes) in the following step. In order to address the procedure specific uncertainties, an MCS routine has been added to the workflow to provide a comprehensive sensitivity and uncertainty analyses. The procedure is based on the evaluation of longitudinal BEPs. Due to the high degree of automation large numbers of BEPs can be analyzed. By a dense arrangement of the individual BEPs, a spatial analysis can be approximated.

The method section introduces the implemented workflow of the tool and contains detailed descriptions of the individual steps and implemented methods. This is followed by a description of the MBES-dataset from lower Rhine, which is used for demonstration purposes. In the results section the resulting bedform parameters and bedload transport rates are presented. The discussion section focuses on the sensitivity of the different procedure specific input parameters. Finally, the key findings are outlined in the conclusions section.

https://doi.org/10.5194/egusphere-2024-579
Preprint. Discussion started: 25 April 2024
© Author(s) 2024. CC BY 4.0 License.

2 Method

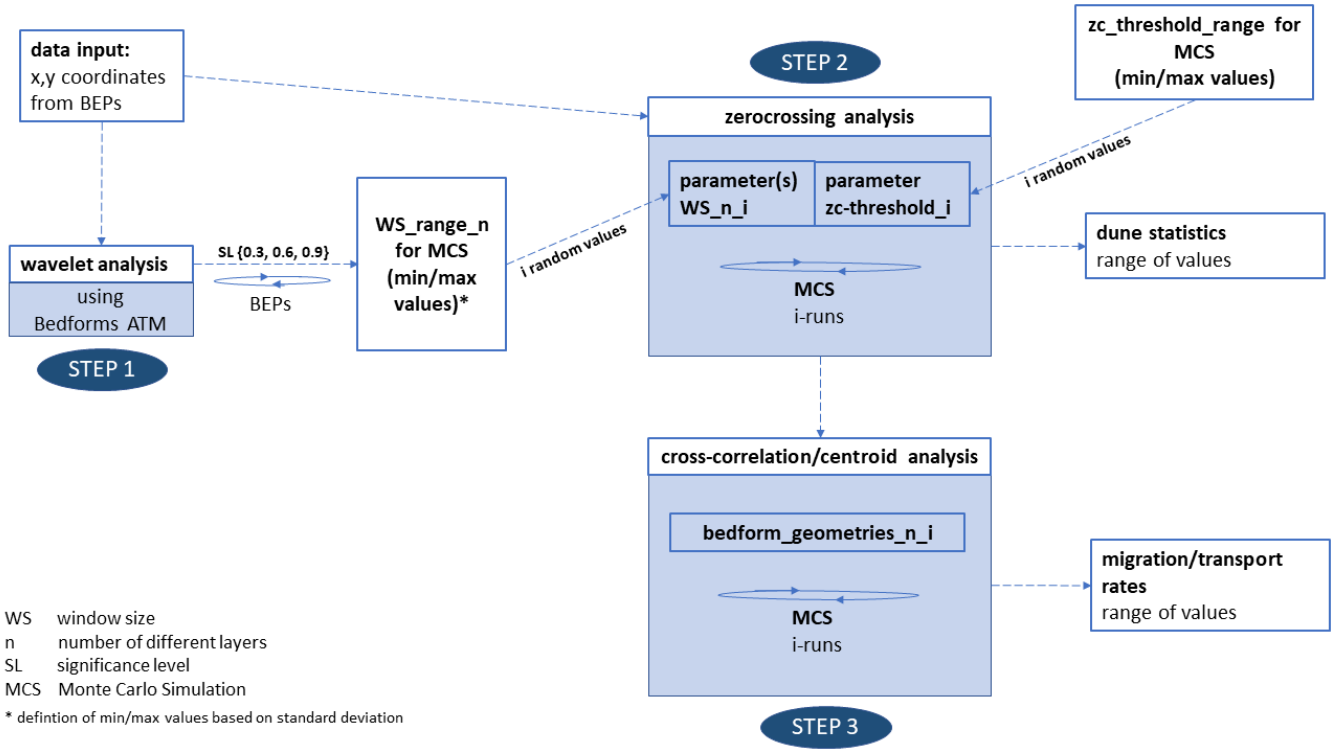

Figure 1: The implemented workflow consists of three steps. For considering the uncertainties associated with the setting of various input parameters, parts of the workflow are performed as an MCS.

Originally, Bedforms-ATM (Guitierrez, 2018) and RhenoBT (Frings et al., 2012) are two separate software tools. For enabling the automated processing of a large amount of datasets, a routine was developed that implements and combines both tools. Figure 1 illustrates the implemented workflow, which consists of the following key points:

- **Input data**: Longitudinal BEPs derived from MBES-data.
- **Step 1 – wavelet analysis**: Bedforms-ATM identifies predominant bedform lengths in a given BEP based on a continuous wavelet transform. This is a required input parameter for step 2.
- **Step 2 – zerocrossing:** The identified predominant bedform lengths are required input parameters (window sizes) for the zerocrossing procedure, based on RhenoBT, which is used to determine bedform geometries. By extending the original algorithm, a data export of tables containing information about individual bedform attributes (e.g. height, length, shape) was implemented, to enable extensive statistical analyses as an optional post-processing routine. In addition, new statistical parameters for the characterization of bedform properties were defined.
- **Step 3 – cross correlation/centroid analysis:** Based on determined bedform geometries, bedform migration rates are calculated using cross-correlation analysis or a newly introduced centroid analysis that is looking at the migration

https://doi.org/10.5194/egusphere-2024-579
Preprint. Discussion started: 25 April 2024
© Author(s) 2024. CC BY 4.0 License.

of the geometrical centroids of individual bedform areas. From a known migration rate bedload transport rates can be derived by considering grain density and porosity.

- **MCS:** At various points in the routine the setting of input parameters is required. This has an impact on the results that is not immediately apparent to the user. Therefore, the calculations are repeated multiple times with different input parameter settings in order to reveal the range of plausible results and to evaluate the level of uncertainties.

2.1 Preprocessing & data preparation

Before the actual analysis, the spatial discretization of the river section under investigation has to be defined. Spatial discretization lateral to the flow direction is given by the distance between the BEPs to each other. The more heterogeneous the investigated bedform field (high spatial variation of bedform dimensions), the denser the arrangement of BEPs should be. In longitudinal direction a division into subsections is mandatory. Later, the statistical parameters (e.g. the average bedform height and length) are calculated per subsection (see Figure 6).

In order to obtain the BEPs from the MBES-data, some hydrographic preprocessing steps are required. Based on the plausibilized raw MBES-data, a geometric modeling is suitable to reduce included measurement uncertainties. Along the considered profile tracks the individual BEPs are derived from the DEMs. A detailed description of hydrographic preprocessing steps can be found e.g. in Lorenz et al. (2021).

2.2 Wavelet analysis

The first step in the procedure is a continuous wavelet transform using Bedforms-ATM. It is performed to identify the predominant wavelengths (interpreted as bedform lengths) in the individual BEPs. The predominant bedform lengths are required input parameters for the zerocrossing procedure that follows in the second step. Wavelet transforms have been used in a variety of applications to analyze riverbed roughness (Nyander et al., 2003) or to discriminate engineering surfaces (Raja et al., 2002). Compared to Fourier methods they are more suitable for signals containing discontinuities. In terms of bedform analysis the so-called Morlet wavelet has appeared to be the most efficient (Guitierrez et al., 2018) and has been used for all analyses in this study. As a result of the wavelet transform, a spectrum is obtained, which indicates the dominance of individual wavelengths in a BEP. Figure 2 shows the so-called wavelet power spectrum for an exemplary BEP. Based on the chosen significance level, the predominant wavelengths are identified. Only those peaks in the wavelet power spectrum that are greater than the global significance are considered. By default, the significance level has to be set by the user. In the shown example (Figure 2) three different significance levels lead to three different results. Accordingly, the workflow has been adapted, so that the analysis is executed three times for each BEP with significance levels of 0.3, 0.6 and 0.9. If multiple predominant wavelengths (equal to several peaks included in the wavelet power spectrum) have been detected, it is assumed that several coexistent layers of bedforms are present. For example, smaller secondary bedforms might be migrating over larger underlying bedforms with (likely) higher migration rates (e.g. Carling et al., 2006; Gilja et al., 2013; Kleinhans et al., 2002). Although the smaller bedforms are usually referred to as secondary and the underlying larger bedforms as primary, in this study, layer 1

https://doi.org/10.5194/egusphere-2024-579
Preprint. Discussion started: 25 April 2024
© Author(s) 2024. CC BY 4.0 License.

describes the upper layer and layer 2 the lower layer of bedforms. This is merely due to the technical procedure, in which the characteristics of the upper layer are determined first and then - if present – those of the lower layer.

The resulting wavelengths from all analyzed BEPs are stored in a table. This table contains the total number of detected wavelengths and is passed to the next step in the routine (zerocrossing procedure) after outliers have been removed. Nevertheless, before carrying out the further calculation steps, it is recommended to check the results from the wavelet analysis for plausibility, to compare them with site-specific knowledge about occurring bedform dimensions and to make manual adjustments if necessary. The most sensitive step is deciding on the number of layers representing features with predominant wavelengths. Due to potential ambiguity of the results, this step is not automated but requires a critical assessment based on the present morphological conditions. In the example shown in Figure 2 different significance levels indicate a different number of layers. This decision has a great impact on all analyses that follow. For instance, the estimated bedload transport rates at the end of the procedure can be over- or underestimated based on the selected number of layers. To make this decision, a visual inspection of the BEPs is recommended. In addition, the calculation of bedform migration rates can be used as validation. If migration rates with high correlation coefficients can be detected for both layers, it can be assumed that the number of layers has been chosen correctly.

Optionally - especially in case of larger-scale gradients of the channel bed (e.g. due to underlying bars) - a detrending of the BEPs can be performed, using robust-spline filter techniques. The algorithm is based on a discrete cosine transform and is used to smooth the initial signal. The degree of smoothing depends on the adjustable s-parameter (for further information refer to Guitierrez et al., 2013).

https://doi.org/10.5194/egusphere-2024-579
Preprint. Discussion started: 25 April 2024
© Author(s) 2024. CC BY 4.0 License.

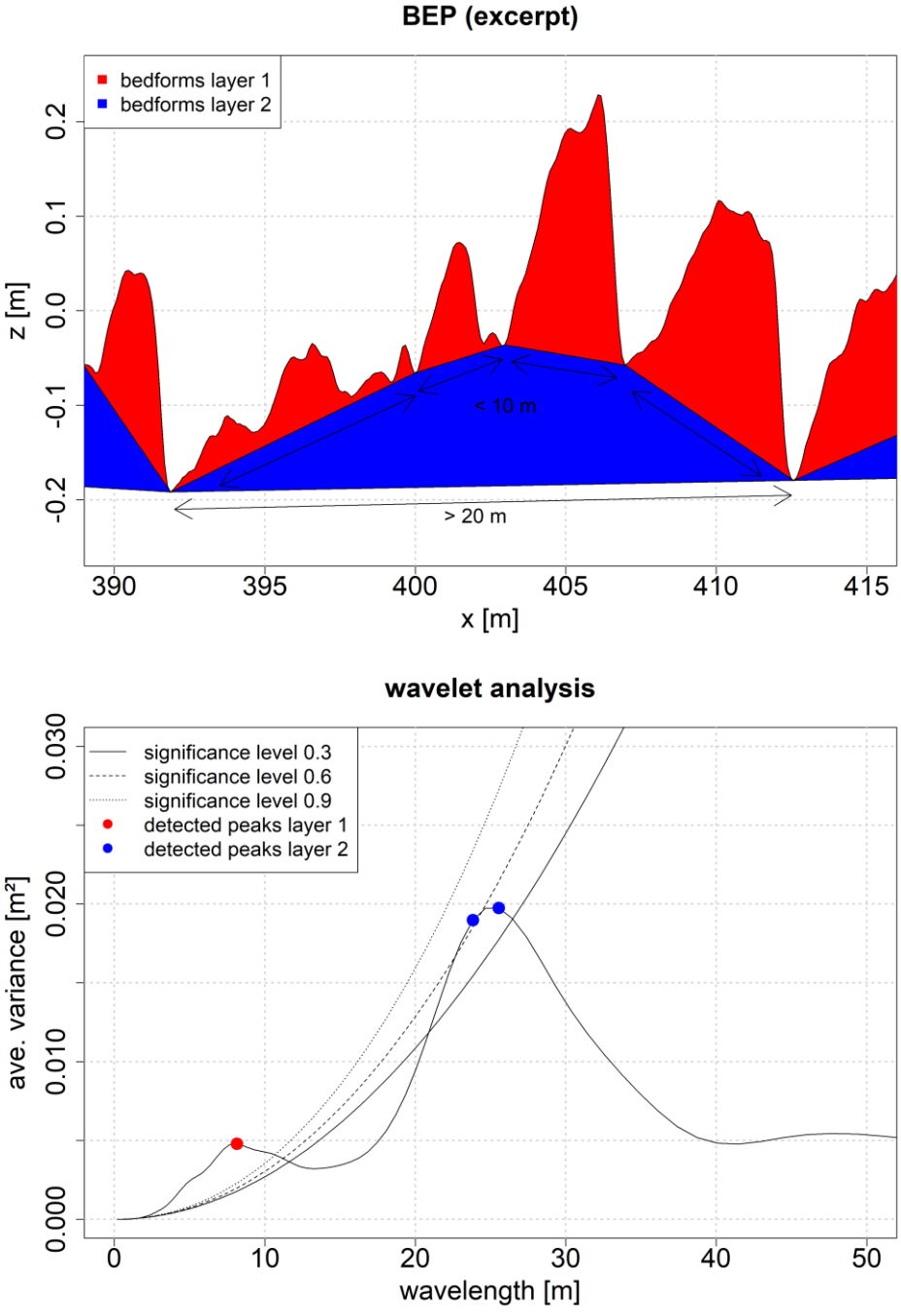

145 **Figure 2: Identifying predominant wavelengths of a BEP by means of wavelet analysis: Depending on the chosen significance level different wavelengths are identified.**

https://doi.org/10.5194/egusphere-2024-579
Preprint. Discussion started: 25 April 2024
© Author(s) 2024. CC BY 4.0 License.

2.3 Zerocrossing procedure

The zerocrossing procedure is adapted from the software RhenoBT, respectively the bedform tracking tool by Van der Mark and Blom (2007). It is a widely used approach for analyzing BEPs with respect to bedform geometries (e.g. Wang et al., 2019; Zomer et al. 2021a). Herein a moving average is calculated over the considered BEP by setting a window size. Ideally, the chosen window size should approximately correspond to the expected bedform length. For this reason, the results from step 1 (Bedforms-ATM) provide the rationale for setting the adequate window size. Figure 3 illustrates the procedure. Based on the moving average the zerocrossings are calculated. The local minima between each two zerocrossings are interpreted as bedform troughs. To limit the effect of small-scale fluctuations in the BEPs a zc-threshold is used, which defines the minimum distance between a bedform trough and the moving average. Only local minima with distances larger than the zc-threshold are considered. At the end of the procedure, usually one or two (depending on the resulting number of layers) baselines are constructed that separate the individual bedform layers from each other. The lowest baseline separates the bedforms from the immobile bed. Based on this separation the individual bedform attributes (height, length and shape) are calculated. If several bedform layers are present, the individual attributes are calculated for each layer separately.

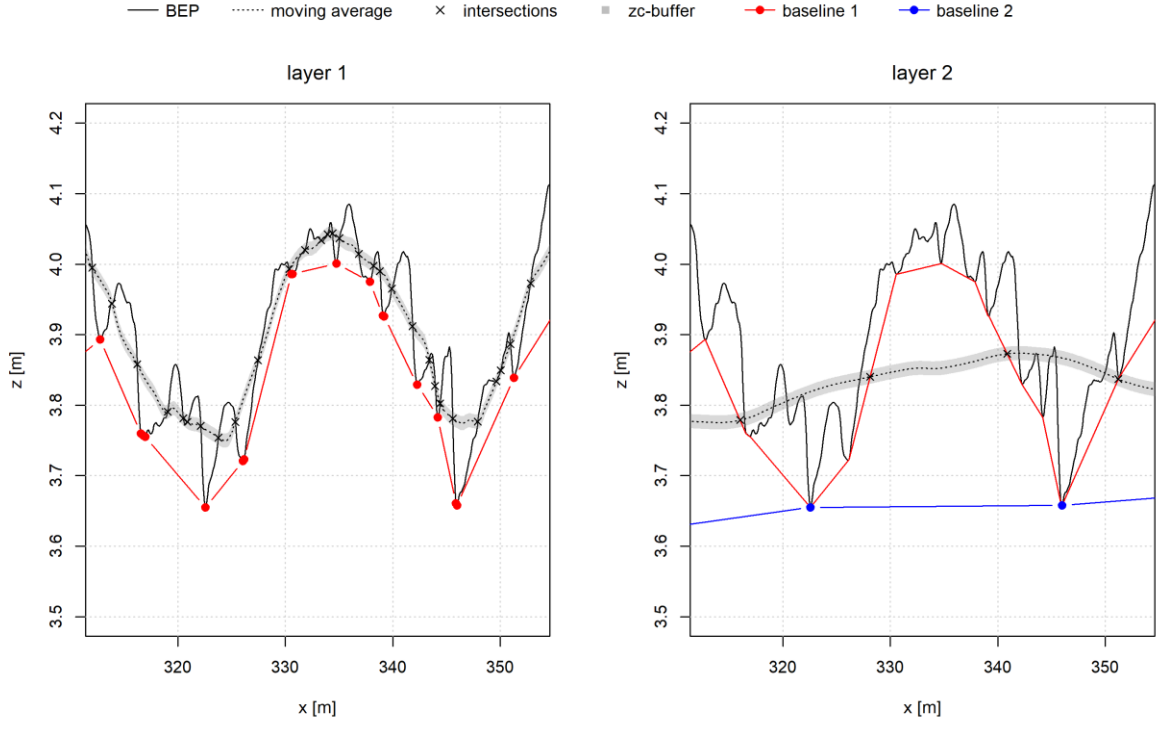

Figure 3: Zerocrossing procedure – Calculating a moving average based on a layer-specific windowsize. Determination of intersections of moving average and BEP (zerocrossing). Local minima between each two zerocrossings (outside the zc-buffer) represent the individual bedform baselines. For layer two the procedure is based on baseline 1 instead of the BEP.

https://doi.org/10.5194/egusphere-2024-579
Preprint. Discussion started: 25 April 2024
© Author(s) 2024. CC BY 4.0 License.

2.4 Bedform statistics

The results of the zerocrossing procedure can be exported as tables, which summarize geometric attributes for each individual bedform as well as the chosen input parameter settings (Table 1), e.g. to enable subsequent statistical analyses as a post-processing routine. The tables are exported for each BEP, subsection, bedform layer and iteration of the MCS.

Table 1: Output from the analysis containing geometrical attributes for each layer

attribute	**definition**
x-position [m]	x-position along the BEP
length [m]	bedform length
height [m]	bedform height
points [-]	number of points
area [m²]	exact bedform area
shape factor [-]	relation between the exact bedform area and the area of the triangle formed by two adjacent bedform troughs and the bedform crest
layer [-]	related bedform layer
iteration [-]	iteration within MCS
windowsize [m]	selected window size
zc-threshold [m]	selected zc-threshold

In accordance to the definition of individual attributes described in Wesseling & Wilbers (2000), bedform length is defined as the length of the line connecting two adjacent troughs, while bedform height is the height of the triangle formed by a crest and its two adjacent troughs. Total height H_{total} is determined by measuring the height of the triangle which is defined by two adjacent troughs of the lowest layer and the maximum of the BEP in between (see Figure 4). Total length L_{total} is equal to the length of the lowest layer. The shape factor is the relation between the exact bedform area and the simplified bedform area resulting from the triangle formed by bedform height and length.

Based on these individual bedform attributes, statistical parameters are calculated to describe average bedform properties in a defined subsection of the BEP. For this purpose, the median is formed over all individual bedform attributes contained in a subsection. Since the determination of these parameters results from the averaging of individual attributes, their significance depends on the number of detected bedforms in the considered subsection. For this reason, another parameter for estimating the total bedform height was implemented, which is independent of the number of identified bedforms. For obtaining the so-called T90-parameter, in each x-value the vertical difference between lowest baseline and the BEP is calculated. Finally, the 90%-percentile of the resulting values is formed within each subsection. Table 2 summarizes the definition of the different parameters.

https://doi.org/10.5194/egusphere-2024-579
Preprint. Discussion started: 25 April 2024
© Author(s) 2024. CC BY 4.0 License.

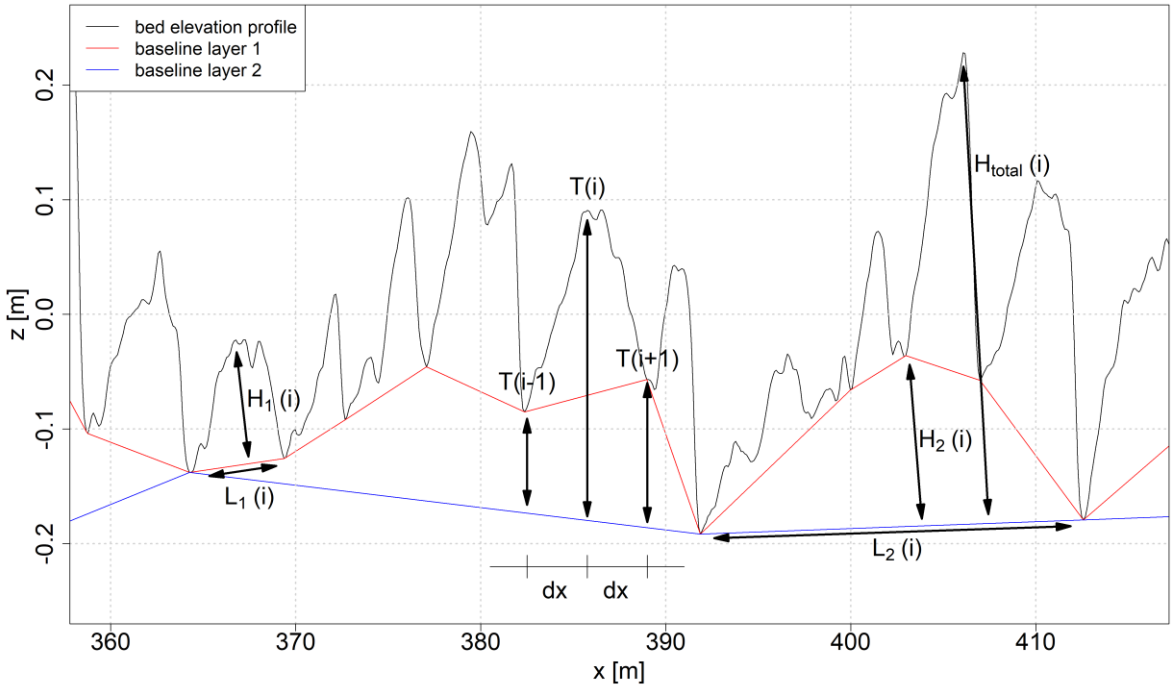

Figure 4: Definition of bedform attributes.

Table 2: Definition of bedform parameters

parameter	Definition	description
T90	90%-percentile of all T(i) along subsection with distance dx	Measure for average total bedform height in a subsection
H_{total}	Median of all H_{total}(i) in a subsection	Measure for average total bedform height in a subsection
H_1	Median of all H_l(i) in a subsection	Measure for average bedform height of layer 1 in a subsection
H_2	Median of all H_2(i) in a subsection	Measure for average bedform height of layer 2 in a subsection
L_1	Median of all L_l(i) in a subsection	Measure for average bedform length of layer 1 in a subsection
L_2	Median of all L_2(i) in a subsection	Measure for average bedform length of layer 2 in a subsection

190

https://doi.org/10.5194/egusphere-2024-579
Preprint. Discussion started: 25 April 2024
© Author(s) 2024. CC BY 4.0 License.

2.4 Estimation of bedform migration & bedload transport

Bedform migration rates can be determined if consecutive measurements over time are available. For this purpose, two different approaches were implemented. By means of a cross-correlation analysis the spatial offset between two consecutive BEPs is identified (Leary and Buscombe, 2019; McElroy and Mohrig, 2009; Van der Mark and Blom, 2007). With the known time offset between each two measurements, migration rates are determined. They can be estimated for the total BEP as well as for the individual layers by using the constructed baselines from the zerocrossing procedure. This can be a decisive aspect in case bedforms of different dimensions occur that migrate with different rates. To consider the upper layer separately the upper baseline is subtracted from the initial BEP. The resulting geometries represent the isolated upper bedforms and are subsequently used in cross-correlation analysis. To consider the lower layer, there are two possible approaches which were evaluated before the final implementation. The first approach is analog to layer one and is based on a subtraction of the lower baseline from the upper baseline. However, preliminary results (not shown here) indicate that correlations are relatively low for this approach. Another option is to directly use the upper baseline in cross-correlation analysis. Both approaches lead to an isolated representation of the lower layer. The second approach has proven to be more efficient and was therefore implemented. In addition to cross-correlation analysis an alternative approach has been developed to better determine the migration rates of small bedforms. The migration of smaller overlaying bedforms decisively contributes to total bedload transport. The resulting quantity may even exceed the transport associated with larger underlying bedforms (Zomer et al., 2021b). This highlights the need for a more detailed analysis of this process. In the presented approach, individual migration rates are obtained - instead of an average migration rate along the entire BEP - by tracking the geometric centroids of individual bedform areas. For two consecutive measurements geometric centroids are calculated for all individual bedform areas obtained from the zerocrossing procedure. Each centroid from the first measurement is assigned to the centroid from the second measurement with the smallest distance in downstream direction. The offset between each pair of centroids corresponds to the individual migration distance. By knowing the time difference between both measurements, migration rates are determined. In order to ensure a correct assignment of corresponding centroids some plausibility check criteria have been defined. For each pair of bedforms, the ratio of bedform length and bedform area is calculated. Assuming that for short measurement intervals bedform geometries should be approximately preserved, a threshold allowing 25% of deformation (concerning length and area) was set. All pairs of bedforms whose ratios exceed this threshold are excluded. The obtained results provide insights into the variability of bedform migration rates along a BEP and can be related to specific geometric attributes. To derive a weighted average migration rate (c_m) from the individual rates for a considered BEP, the products of individual migration rate (c_i) and corresponding bedform length (L_i) are summed up and divided by the total length of the BEP (L_{BEP}).

$$c_m = \frac{\sum c_i \cdot L_i}{L_{BEP}} \quad \textbf{(1)}$$

https://doi.org/10.5194/egusphere-2024-579
Preprint. Discussion started: 25 April 2024
© Author(s) 2024. CC BY 4.0 License.

The method is only suitable for short measurement intervals within which the migration distance is much smaller than the bedform length (dx << L). For longer intervals, successive deformation as well as occurring bedform splitting and merging processes make a correct assignment increasingly difficult. However, this is also true for cross-correlation analysis. This new approach is also rather unsuitable for underlying larger bedforms, since for short intervals the spatial offset is too small to enable a precise assignment (approaching the limit in terms of measurement accuracy) whereas for large intervals deformation already has too much influence on the calculation of the geometric centroids.

Figure 5 illustrates the two approaches for a pair of BEPs selected for demonstration purpose. The upper plot shows the results from cross-correlation analysis and the shifted BEPs. The lower plot shows the calculated individual offsets from centroid analysis. In the following cross-correlation analysis is referred to as method 1 and centroid analysis as method 2.

https://doi.org/10.5194/egusphere-2024-579
Preprint. Discussion started: 25 April 2024
© Author(s) 2024. CC BY 4.0 License.

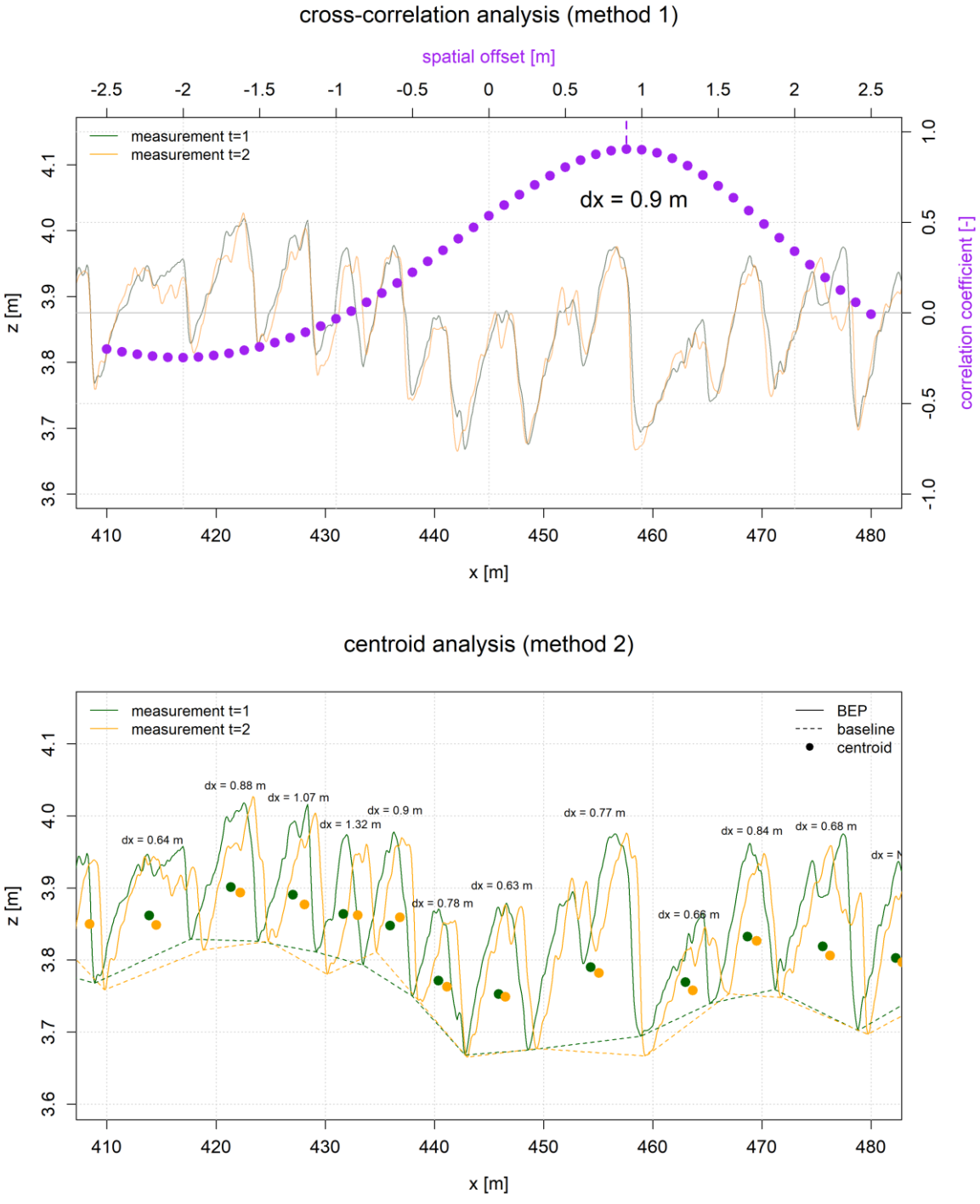

Figure 5: Calculation of bedform migration based on cross-correlation analysis (upper plot) and by comparing the geometrical centroids individual bedform areas (lower plot).

https://doi.org/10.5194/egusphere-2024-579
Preprint. Discussion started: 25 April 2024
© Author(s) 2024. CC BY 4.0 License.

Based on the obtained migration rates - and by considering porosity and density, bedload transport rates (given in g s^{-1} m^{-1}) can be estimated. The approach by Ten Brinke et al. (1999) includes migration rate c (m s^{-1}), density ρ (g cm^{-3}), porosity n (-), bedform height H (m) and shape factor S (-).

$$q_b = c \cdot H \cdot S \cdot 0.5 \cdot \rho \cdot (1 - n) \quad \textbf{(2)}$$

The shape factor is the relation between the exact bedform area and the area of the triangle formed by bedform height and length (S = H·L·0.5). Since during the procedure the exact area of each single bedform is calculated, shape factor and bedform height can be replaced. For this purpose, the sum A (m^2) of the individual bedform areas is used. This way, no averaging of bedform properties along the BEP is necessary. To obtain the correct unit, the result must be divided by the total length of the BEP.

$$q_b = c \cdot \frac{A}{L_{BEP}} \cdot \rho \cdot (1 - n) \quad \textbf{(3)}$$

Both, the calculation of bedform migration and bedload transport are also part of the MCS as the results depend on the obtained bedform geometries in step 2.

2.5 Monte Carlo simulation

According to Figure 1, steps 2 and 3 of the dunetracking tool are executed as a Monte Carlo Simulation in order to address the possible range of results and the correspondent level of uncertainty. Concerning step 1, the results of the wavelet analysis (Bedforms-ATM) provide an orientation for setting the window sizes in step 2 (zerocrossing procedure according to RhenoBT). For each BEP, the wavelet analysis is performed three times with significance levels of 0.3, 0.6 and 0.9. The resulting bedform lengths from all analyzed BEPs are stored in a table. This table now contains the total number of detected bedform lengths. In order to exclude outliers, mean value and standard deviation are calculated for each layer. The final range of considered bedform lengths for each layer results from twice the standard deviation around the mean value (denoted as 'WS_range_n' in Figure 1). These steps ensure an automated and a reproducible procedure. The obtained ranges of bedform lengths are then used in the following zerocrossing procedure.

For applying the zerocrossing procedure in step 2, the user-defined input are the following parameters: i) the respective window sizes for calculating the moving average of the individual bedform layers (denoted as 'WS_n_i' in Figure 1), and ii) the zc-threshold (denoted as 'zc-threshold_i' in Figure 1). Within a given range, random values are generated for each parameter according to a uniform distribution. Concerning the window sizes, the ranges of bedform lengths resulting from the wavelet analysis are used ('WS_range_n_for MCS'). For zc-threshold there is a lack of objective criteria, but globally, it must not be

https://doi.org/10.5194/egusphere-2024-579
Preprint. Discussion started: 25 April 2024
© Author(s) 2024. CC BY 4.0 License.

greater than the minimum expected bedform height. The random values for i) und ii) are generated once and are then used for all BEPs and all repeated measurements, in order to ensure comparability. Using all available sets of generated random values results in multiple representations of the bedform geometries for each BEP (denoted as 'bedform_geometries_n_i' in Figure 1). All these representations are then used to calculate bedform migration and bedload transport rates in step 3, in which two consecutive measurements over time are always considered in pairs. To ensure comparability, only pairs of representations of the bedform geometries with identical parameter settings are considered.

By performing this MCS, the possible range of results can be quantified for all steps of the procedure. At the same time, the various statistical parameters can be examined with respect to their robustness. For examining the behavior of each input parameter separately, additional runs can be executed in which only one parameter is varied at a time while all the other parameters are kept constant. The number of iterations is freely selectable. The higher the number the more robust the estimates. On the other hand, a very high number of iterations leads to longer computational times. With respect to the analyses shown here, 100 iterations per BEP were performed.

3 Dataset

An MBES-dataset of the Lower Rhine in Germany was chosen as a testcase to demonstrate the dunetracking tool. The dataset was obtained during a field measurement carried out by the Federal Waterways and Shipping Administration in February 2020. All hydrographic processing steps (e.g. plausibility checks, geometric modelling, extraction of longitudinal BEPs from spatial data) were carried out by the Federal Institute of Hydrology.

The study area is located close to Emmerich at Rhine-kilometer 860.0 to 860.5 and covers 500 meters in length and about 200 meters in width (see Fig. 5). The section is characterized by a mixed sand and gravel bed with grain sizes in the order of 6 mm (D50). According to BfG (2011) grain density was assumed to be 2.603 g cm^{-3} and for porosity a value of 0.30 was selected. The measurements were taken on consecutive days at medium to high flow conditions with discharges ranging from 4000 to 4200 m^3 s^{-1} and depth-averaged flow velocities of about 1.9 m s^{-1} in the main channel. The total area covered with bedforms was measured four times with intervals between three and 24 hours. Additional measurements were taken along a single profile track in the center of the bedform field at shorter intervals, allowing a more detailed analysis of bedform migration and bedload transport.

Table 3 shows all measurements performed during the campaign. In order to expand the data basis with respect to bedform migration and bedload transport, not only directly consecutive measurements but all possible combinations (for dt > 0) are considered. The 10 available detailed measurements thus result in $\binom{10}{2} = 45$ possible combinations (see Appendix A).

https://doi.org/10.5194/egusphere-2024-579
Preprint. Discussion started: 25 April 2024
© Author(s) 2024. CC BY 4.0 License.

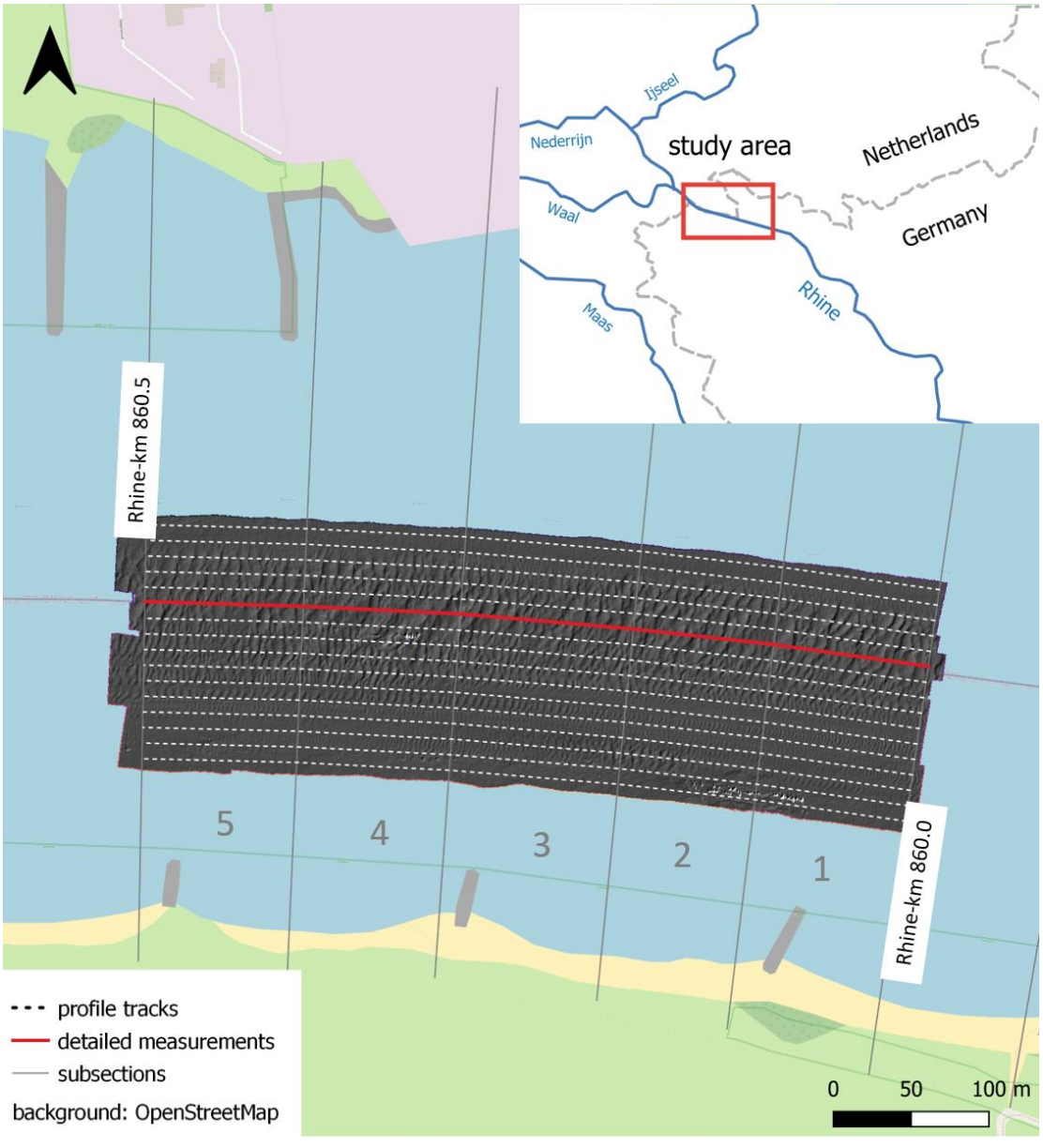

295

Figure 6: Study area near Emmerich (Rhine-km 860.0 to 860.5). Spatial discretization into 16 profile tracks lateral to flow direction and into 100-meter subsections in longitudinal direction. Base map is from © OpenStreetMap contributors 2023. Distributed under the Open Data Commons Open Database License (ODbL) v1.0.

https://doi.org/10.5194/egusphere-2024-579
Preprint. Discussion started: 25 April 2024
© Author(s) 2024. CC BY 4.0 License.

Table 3: Performed measurements during field campaign

No.	date	time (MET)	measured area	Δt [h][1]
1	17 February 2020	09:35–10:41	total bedform field	-
2	18 February 2020	09:35–10:21	total bedform field	24.0
3	18 February 2020	12:48–13:31	total bedform field	3.2
4	19 February 2020	09:52–10:36	total bedform field	21.1
5	17 February 2020	11:17–11:24	single profile	-
6	17 February 2020	12.13–12:20	single profile	0.9
7	18 February 2020	08:46–08:54	single profile	20.6
8	18 February 2020	10:29–10:37	single profile	1.7
9	18 February 2020	10:41–10:48	single profile	0.2
10	18 February 2020	11:05–11:13	single profile	0.4
11	18 February 2020	11:57–12:04	single profile	0.9
12	18 February 2020	13:36–13:43	single profile	1.6
13	19 February 2020	09:24–09:32	single profile	19.8
14	19 February 2020	11:12–11:20	single profile	1.8

Hydrographic processing was performed according to Lorenz et al. (2021). The measurement data were plausibilized and modelled to a regular grid with a point spacing of 10 cm. Longitudinal BEPs were derived from the created DEM. The measured bedform field was subdivided into 16 BEPS with a lateral distance of 10 m to each other (see Figure 6). Figure 7 shows the derived normalized BEPs. Largest bedforms are located between BEP 8 and BEP 14 covering the entire length of the study area. Between BEP 3 and BEP 7 smaller bedforms are located, occurring only occasionally in individual subsections. Along BEP 1, 2, 15 and 16 no significant bedforms were measured.

[1] time difference to previous measurement

https://doi.org/10.5194/egusphere-2024-579
Preprint. Discussion started: 25 April 2024
© Author(s) 2024. CC BY 4.0 License.

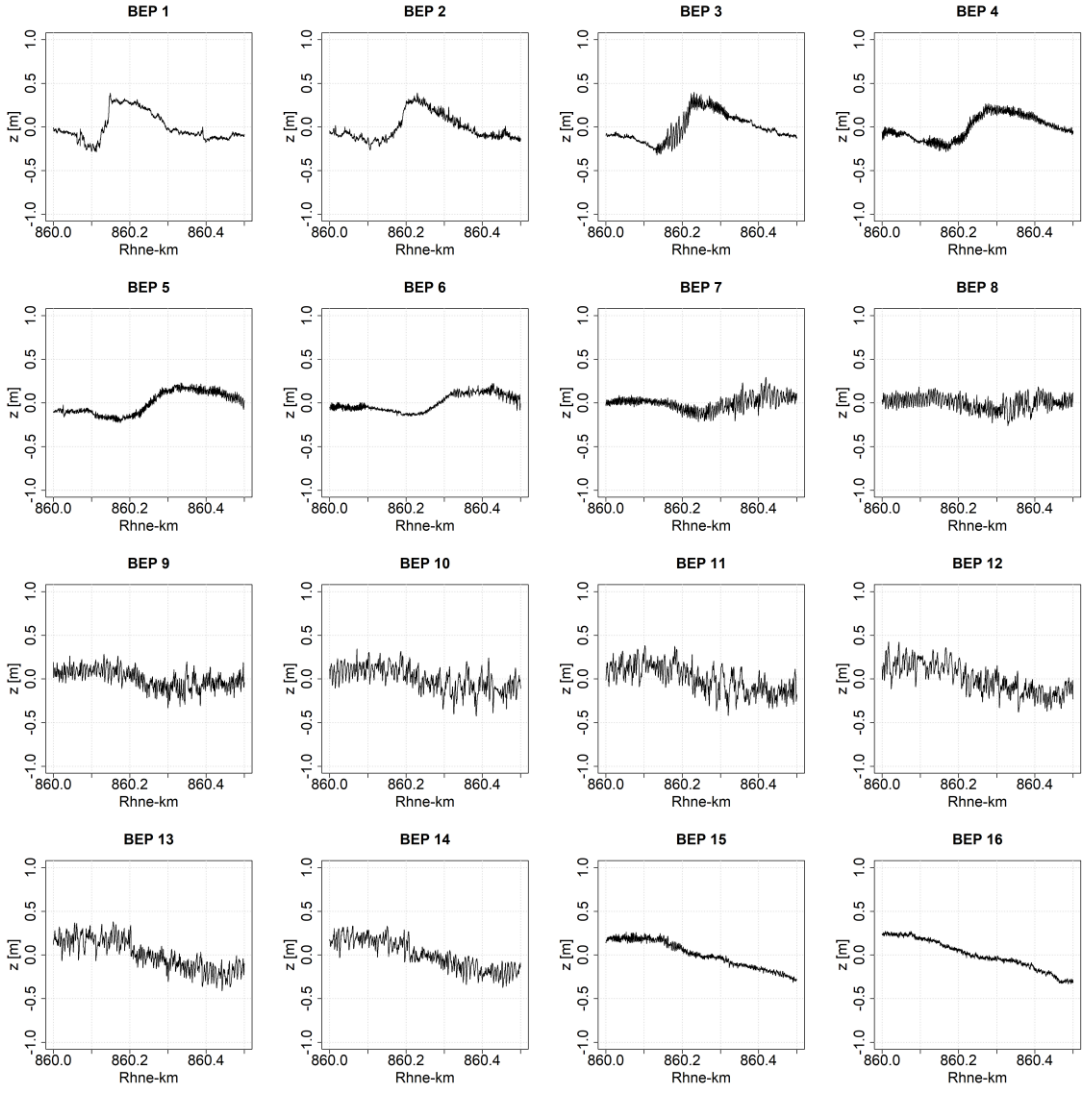

Figure 7: Normalized BEPs derived from MBES-data of the first measurement from 17 February 2020.

4 Results

4.1 Wavelet analysis

315 Figure 8 shows the identified predominant wavelengths calculated in the first step (wavelet analysis with Bedforms-ATM). Wavelengths of the upper layer (layer 1) slightly increase from left to right reaching a maximum of 13 meters. Near the boundaries of the study area no wavelengths could be identified (BEPs 1 & 2 as well as 15 & 16). In the center of the bedform field, a second layer of bedforms with larger wavelengths in the order of 25 meters was detected. A visual comparison of the results with the BEPs shown in Figure 7 confirms the plausibility of the results. The resulting migration rates from cross-

https://doi.org/10.5194/egusphere-2024-579
Preprint. Discussion started: 25 April 2024
© Author(s) 2024. CC BY 4.0 License.

correlation analysis (see Sec. 4.3) will also verify the assumption of two separate layers. The detected wavelengths are based on all four measurements of the total bedform field (see Table 3) and on different settings of the significance level which were 0.3, 0.6 and 0.9.

To focus the further analyses and in order to demonstrate the use of the presented dunetracking tool, only the center of the bedform field (BEP 8 to 14) was considered. Along the other BEPs, either only very small bedforms occur or bedforms only cover a limited section. The ranges of respected wavelengths are defined by twice the standard deviation around the mean value (see Sect. 2). All detected wavelengths were within the specified ranges.

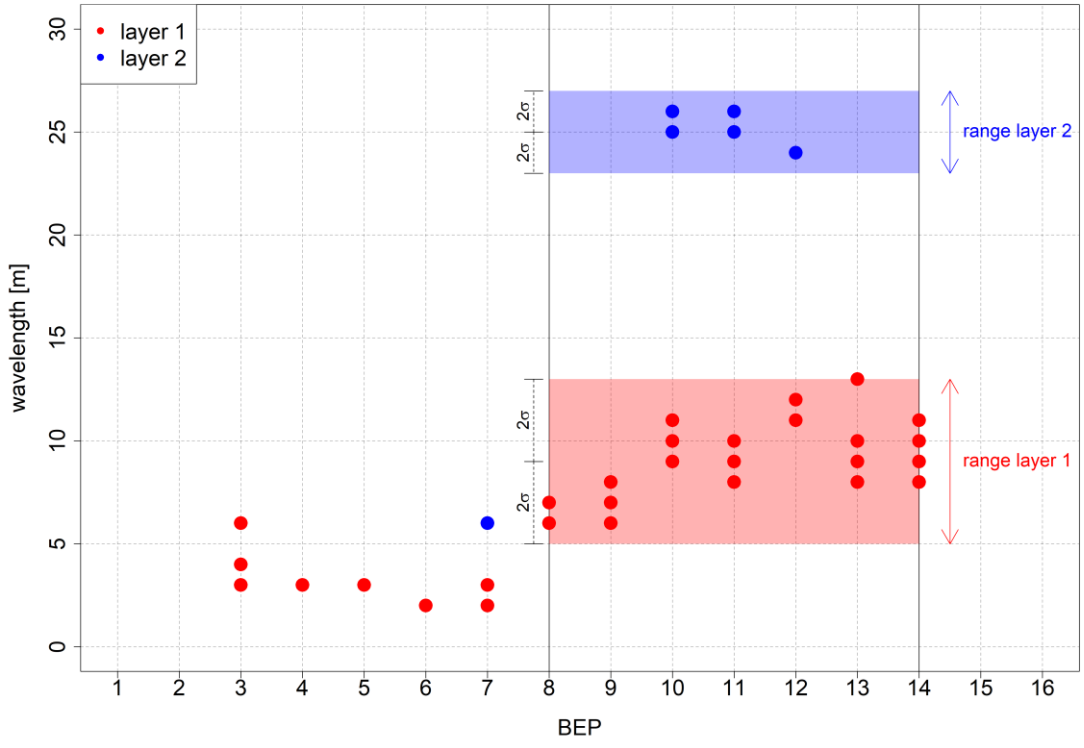

Figure 8: Derivation of the ranges of window sizes for the zerocrossing procedure from the identified predominant wavelengths in individual BEPs by means of wavelet analysis.

4.2 Bedform geometries

The wavelet analysis determines the range of values for the input parameter window size in the zerocrossing procedure (step 2). For each BEP, 100 iterations were performed with varying settings (MCS). Window sizes for layer 1 were varied between five and 13 meters while window sizes for layer 2 were varied between 23 and 27 meters (according to 2σ in Figure 8). The

https://doi.org/10.5194/egusphere-2024-579
Preprint. Discussion started: 25 April 2024
© Author(s) 2024. CC BY 4.0 License.

setting of zc-threshold, the second input parameter, was varied between 0.5 and 5 cm, which are assumed to be smaller values than the expected minimum bedform height. At the same time, the derivation of even smaller structures would reach the limits of measurement accuracy. Based on the specified ranges for each input parameter, random values are generated according to a uniform distribution. Figure 9 shows the bedform parameters obtained from 100 iterations. The parameters were averaged along each BEP. With respect to bedform geometries temporal changes can be neglected due to the short time intervals between the individual measurements. Therefore, only the first measurement (no. 1 in Table 3) is considered in this context.

Regarding total bedform height, the T90 parameter remains nearly constant over all iterations for all BEPs, whereas the H_{total}-parameter has a higher scattering with a maximum range of about 5 cm (Fig. 8). The mean for both parameters takes a maximum in BEP 11 (values of 33 and 35 cm). Considering the individual bedform layers, bedforms of layer 2 appear to be slightly lower (mean values range from 15 cm to 19 cm for H_1 and from 5 cm to 15 cm for H_2) but much longer than those of layer 1 (mean values range from 5 m to 6 m for L_1 and from 17 m to 22 m for L_2). Bedform lengths appear to behave very sensitive with respect to varying input parameter settings. Mean lengths of layer 1 remain nearly constant over all BEPs with a maximum total range of 4 m. Lengths of layer 2, however, show a maximum total range of up to 10 m in BEP 12, which corresponds to 50 % of the mean length. It should be noted that spatial averaging (over the cross section) can lead to a stabilization and thus to a decreased scattering of the results.

https://doi.org/10.5194/egusphere-2024-579
Preprint. Discussion started: 25 April 2024
© Author(s) 2024. CC BY 4.0 License.

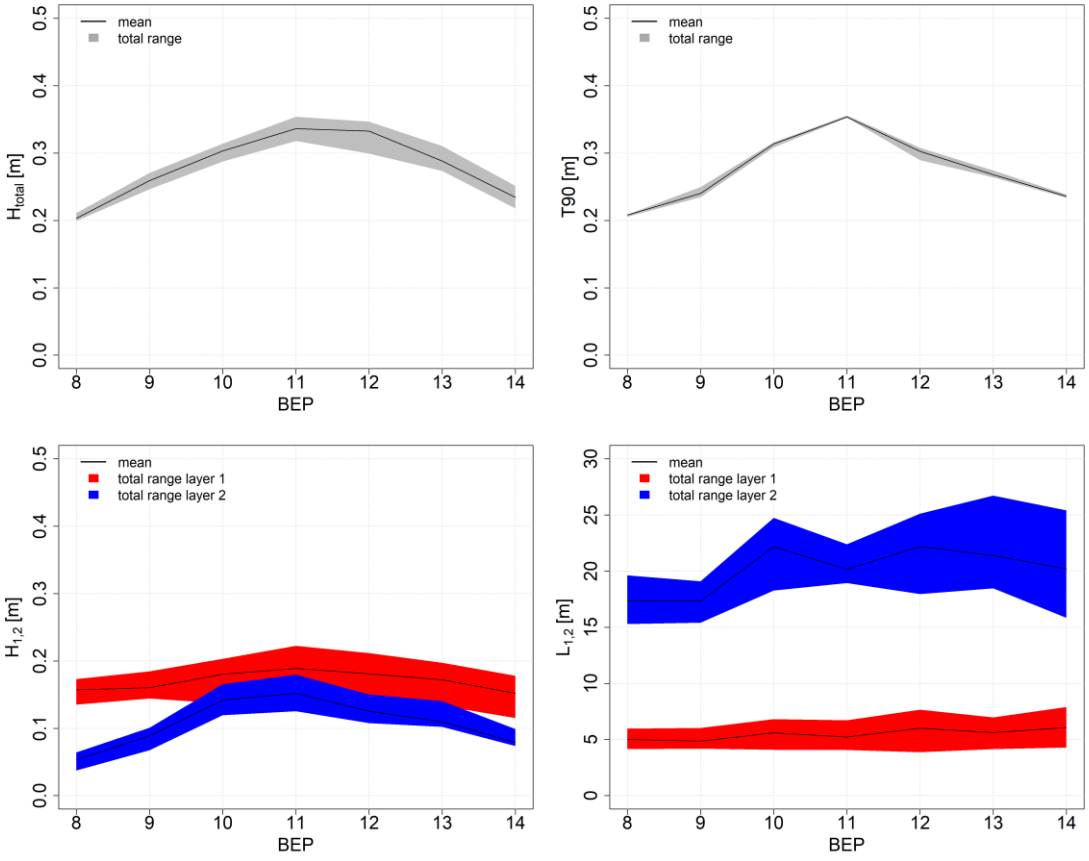

Figure 9: Resulting bedform parameters of the Monte Carlo Simulation.

4.3 Bedform migration & bedload transport

To enable the calculation of bedform migration rates, repeated measurements were performed during the campaign, with a minimum time interval of 3.2 hours between two successive measurement for the entire bedform field. These intervals turned out to be too long, in order to track the smaller and hence faster migrating bedforms of layer 1. Therefore, only the detailed measurements of the single BEP (no. 5-14 in Table 3) are considered for the analysis of migration rates. Here, intervals are much shorter and start from 0.2 h. Based on the 10 available measurements, 45 pairwise combinations can be analyzed (see Appendix A, Table A1). Migration rates were calculated using two different approaches as introduced in Sect. 2.

Figure 10 shows the correlation coefficients derived from cross-correlation analysis (method 1) as a function of time interval dt between two measurements. Correlation coefficients are shown here for the total BEP as well as for the individual layers. For considering the individual layers the constructed baselines from the MCS were used (see Sect. 2). Accordingly, for each measurement results from 100 iterations are available. Correlation coefficients obviously decrease with increasing measurement interval due to the deformation of bedforms. However, correlation coefficients of layer 2 and the total BEP remain above a value of 0.7 even after 20 hours. Concerning the smaller bedforms of layer 1 correlation coefficients decrease

https://doi.org/10.5194/egusphere-2024-579
Preprint. Discussion started: 25 April 2024
© Author(s) 2024. CC BY 4.0 License.

much more rapidly and drop below a value of 0.5 after less than two hours, highlighting that longer time intervals between measurements are unsuitable for tracking these bedforms.

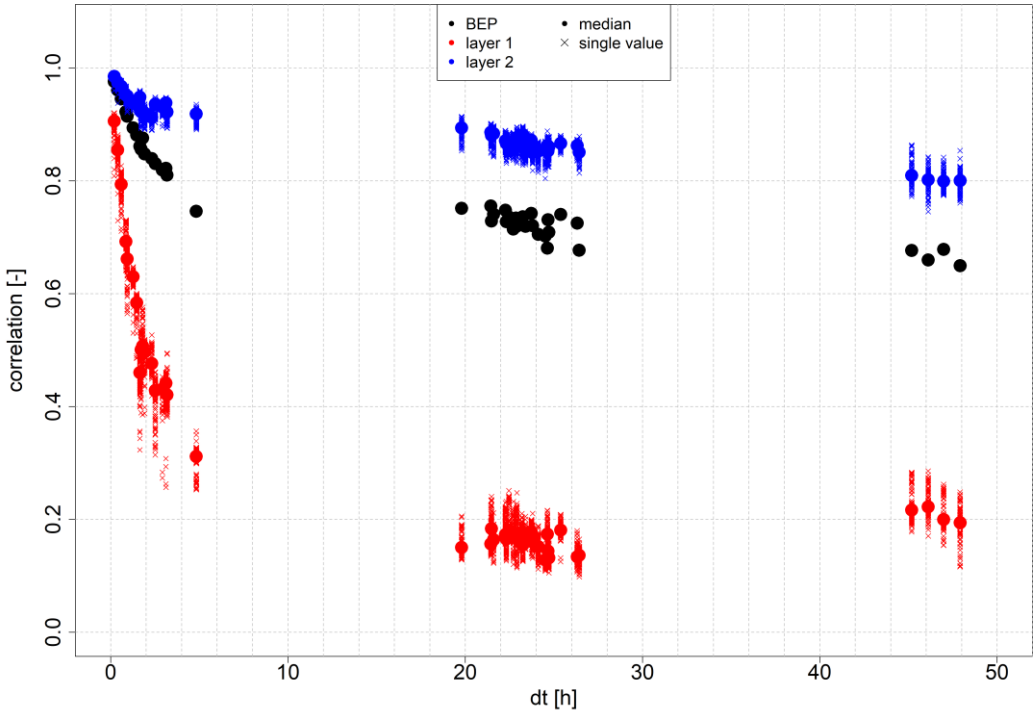

Figure 10: Correlations coefficients from cross-correlation analysis (method 1) as a function of time interval between successive measurements.

Figure 11 summarizes the migration rates for all 45 possible combinations of measurements. Results with correlation coefficients smaller than 0.5 are indicated by transparent symbols. These are excluded from the calculated medians. For layer 1 median migration rates fluctuate between 1.5 and 2.2 m h^{-1}. For all measurement pairs above no. 12, the correlation coefficients drop below the 0.5 threshold value, thus no reliable results are available for measurement intervals longer than two hours. For layer 2, median migration rates fluctuate between 0.1 and 0.8 m h^{-1}. For dt > 20 hours fluctuations are much lower. Concerning migration rates of the total BEPs (without discriminating between individual layers), results for short measurement intervals are close to those of layer 1, while results for longer measurement intervals are close to those of layer 2, depending on which process is dominant. This highlights the need for discriminating between the individual layers in order to make precise statements about migration rates, as they highly depend on bedform dimensions. Both, migration rates for layer 1 as well as for the BEP decrease with increasing measurement intervals. This effect can probably be attributed to the fact that small bedforms tend to migrate faster, but at the same time can only be reliably tracked for very short measurement intervals. For small dt, the migration of small bedforms has a significant effect on the cross-correlation analysis (and thus on the determination of the best fitting spatial offset). With increasing dt, deformation of bedforms increases so that the smallest

https://doi.org/10.5194/egusphere-2024-579
Preprint. Discussion started: 25 April 2024
© Author(s) 2024. CC BY 4.0 License.

bedforms are no longer traceable and the average migration rate decreases. This effect can also be seen by looking at the results obtained from method 2, which will be presented in the following.

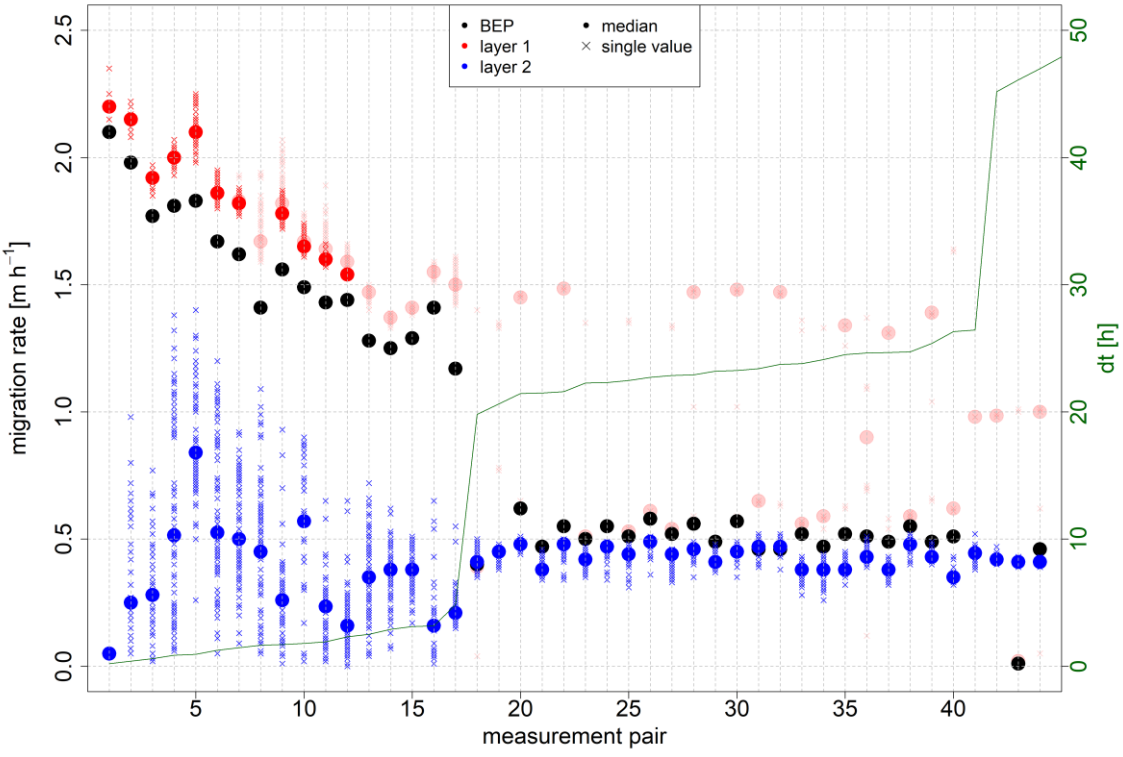

Figure 11: Calculated migration rates for all respected measurement pairs by means of cross-correlation analysis (method 1, transparent symbols represent values with correlations smaller than 0.5).

Figure 12 displays the results from the second approach looking at the migration of geometrical centroids of individual bedforms (centroid analysis, method 2). A Lowess smoothing with a smoothing span of 0.5 was performed to investigate the relationship between bedform area and migration rate. For short measurement intervals (measurements carried out on the same day with dt < 5 h) migration rates vary between 0 m h^{-1} and 8 m h^{-1}. At the same time, at least for layer 1, a steep decline of migration rates can be seen as bedform area increases. For longer measurement intervals (measurements carried out on subsequent days with dt > 19 h), a clear relation is no longer recognizable.

https://doi.org/10.5194/egusphere-2024-579
Preprint. Discussion started: 25 April 2024
© Author(s) 2024. CC BY 4.0 License.

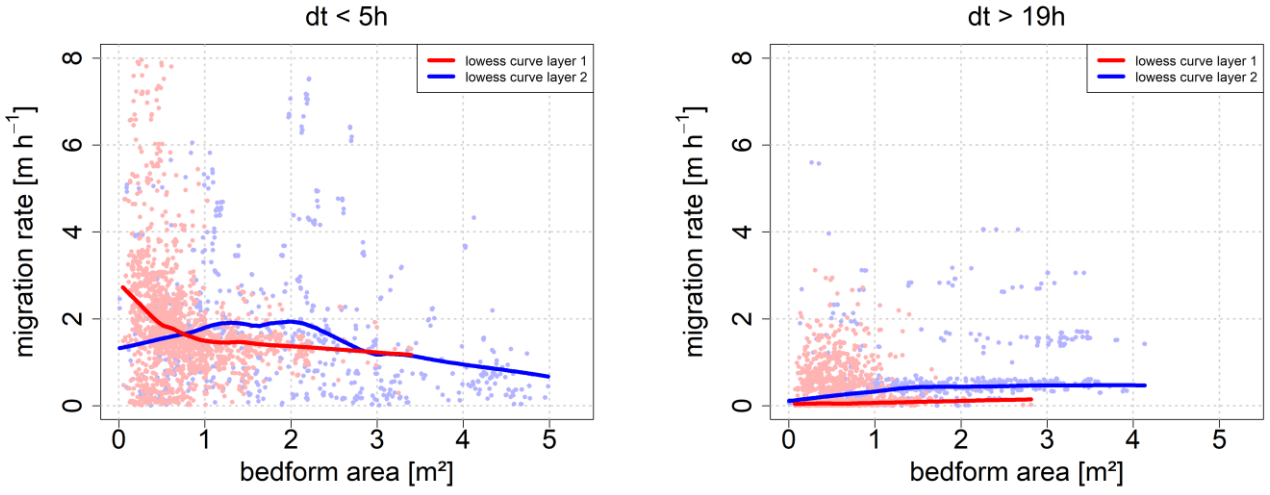

Figure 12: Migration rates of individual bedforms by means of centroid analysis (method 2) for measurements carried out on the same day (left) and for measurements carried out on subsequent days (right). The lowess curve was calculated based on a smoother span with a value of 0.5.

As described in Sect. 2, the results are filtered by the defined quality criteria considering the geometrical similarity of corresponding bedforms from two measurements. For layer 1, the number of traceable bedforms strongly decreases as the measurement interval dt increases (see Figure 13). For this reason, the results for longer measurement intervals should be assessed with particular caution. In contrast, the number of traceable bedforms of the second layer is low for all measurement pairs and does not change significantly as dt increases. As mentioned in Sect. 2, this approach is rather unsuitable for tracking large and slowly migrating bedforms. Very small spatial offsets for short measurement intervals and increasing deformation for longer measurement intervals make the exact identification of the geometrical centroids particularly difficult. However, another reason for the smaller number of traceable bedforms for layer 2 can be found in the distribution of larger bedforms along the BEPs. While the smaller bedforms of layer 1 can be found along the entire BEP, larger bedforms of layer 2 are only present in certain subsections and are not covering the total length of the BEP.

https://doi.org/10.5194/egusphere-2024-579
Preprint. Discussion started: 25 April 2024
© Author(s) 2024. CC BY 4.0 License.

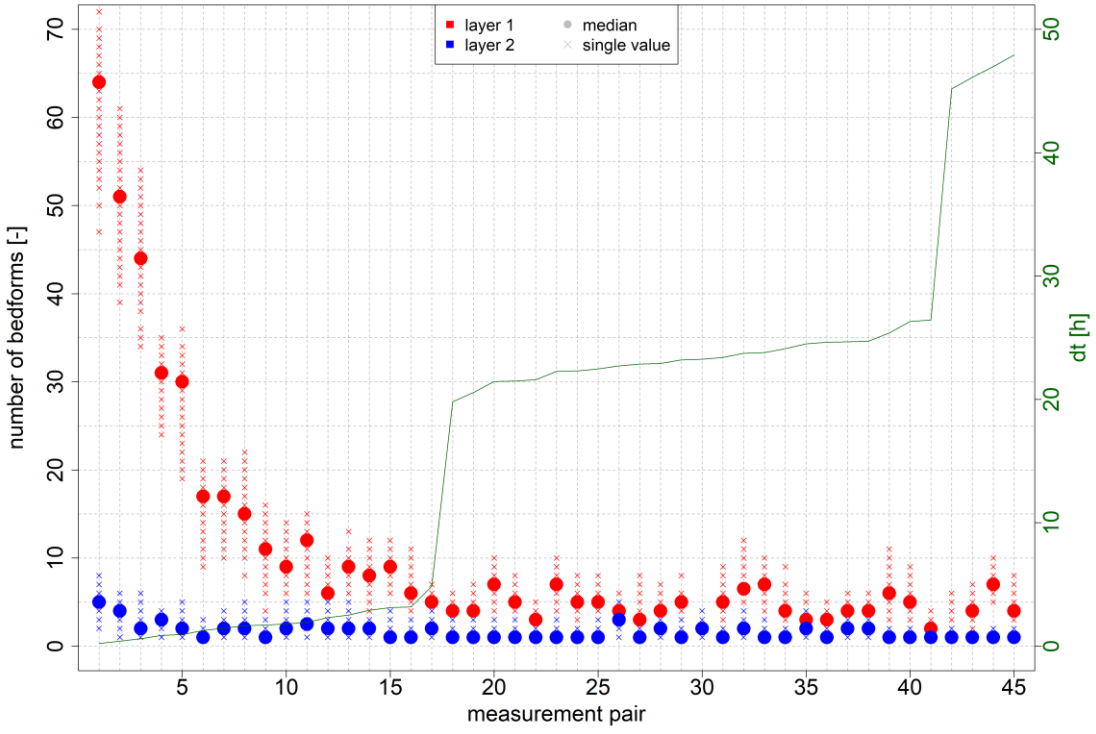

Figure 13: Number of traceable bedforms depending on measurement interval (centroid analysis, method 2).

Figure 14 shows weighted average migration rates along the BEP for each measurement pair. The MCS was preset to generate 100 results for each measurement pair. After filtering the results based on the established quality criteria, outliers exceeding a 95% percentile were removed. In total, fluctuations are higher compared to method 1. For layer 1 median migration rates vary between 1 m h^{-1} and 2 m h^{-1} for short measurement intervals (dt < 5h). For longer measurement intervals values vary between 0 m h^{-1} and 0.5 m h^{-1}. As shown in Figure 13 the number of traceable bedforms drastically decreases with increasing dt, which is why only the results for very short measurement intervals are of sufficient quality. Here, the results are quite comparable to those of method 1 in Figure 11. Again, migration rates decrease with increasing dt. As explained above, this effect is caused by the decreasing number of traceable bedforms with small areas and high migration rates. For layer 2 the number of traceable bedforms is constantly low (≤ 5). For small measurement intervals fluctuations are very high. As mentioned before, the identification of geometrical centroids is subject to great uncertainties concerning large bedforms and short measurement intervals. For longer measurement intervals, however, migration rates are again comparable to those obtained from method 1 and vary from 0.1 to 0.6 m h^{-1}.

https://doi.org/10.5194/egusphere-2024-579
Preprint. Discussion started: 25 April 2024
© Author(s) 2024. CC BY 4.0 License.

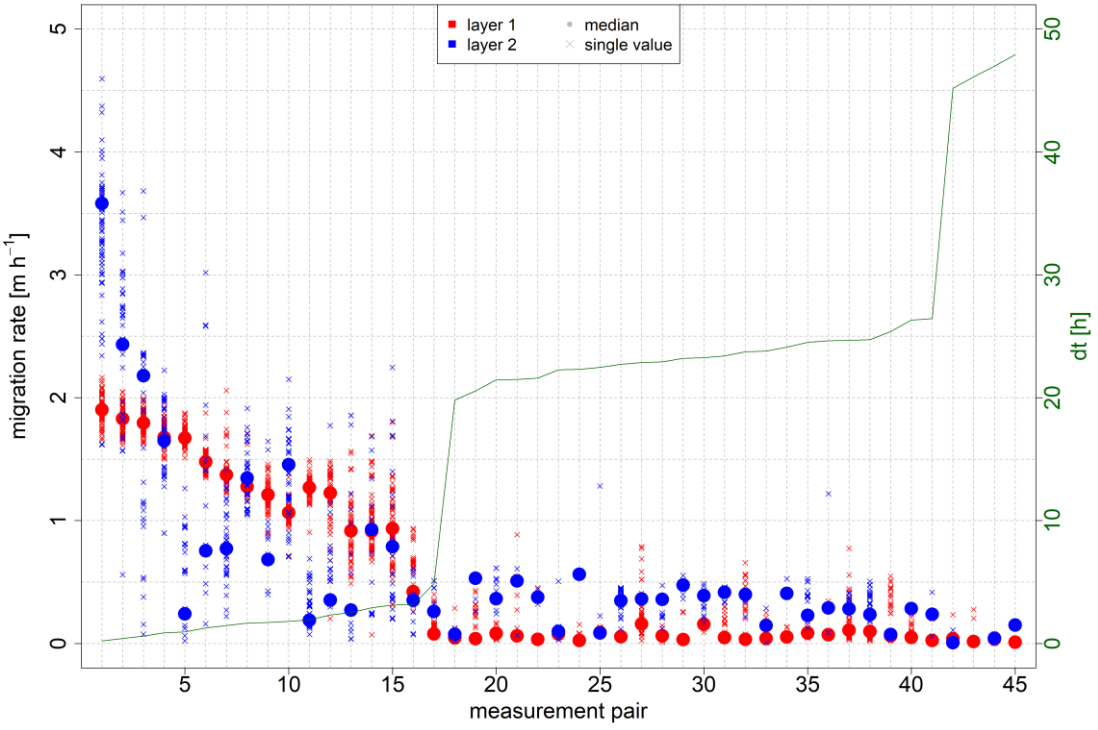

Figure 14: Calculated migration rates for all respected measurement pairs by means of centroid analysis (method 2).

Based on the migration rates calculated by the two methods, bedload transport rates were estimated using Eq (3. As just shown, the time interval between two measurements has a strong impact on resulting migration rates and hence on estimated bedload transport rates. Smaller bedforms of layer 1 can only be tracked accurately by using short intervals while longer intervals are more suitable for larger bedforms of layer 2. For this reason, only measurement intervals shorter than two hours were considered for the estimation of bedload transport for layer 1, whereas only measurement intervals longer than 19 hours (measurements carried out on different days) were considered for layer 2. For estimating the total transport, the quantities for both layers were summed up. Figure 15 shows estimated bedload transport rates and their ranges resulting from the different input parameter settings within the MCS for both methods. Again, the results obtained from centroid analysis are subject to a greater uncertainty with total bedload transport rates fluctuating within a range of about 60 g s^{-1} m^{-1} (corresponding to more than 50% in relation to the median). In comparison those obtained from cross-correlation analysis only fluctuate within a range of about 40 g s^{-1} m^{-1} (corresponding to about 30% in relation to the median). Median values, however, are in the same order of magnitude for both methods. Further on, both methods indicate that bedload transport associated with the bedforms of layer 1 accounts for nearly 90% of the total transport, while bedload transport associated with the bedforms of layer 2 accounts for only slightly more than 10 %.

https://doi.org/10.5194/egusphere-2024-579
Preprint. Discussion started: 25 April 2024
© Author(s) 2024. CC BY 4.0 License.

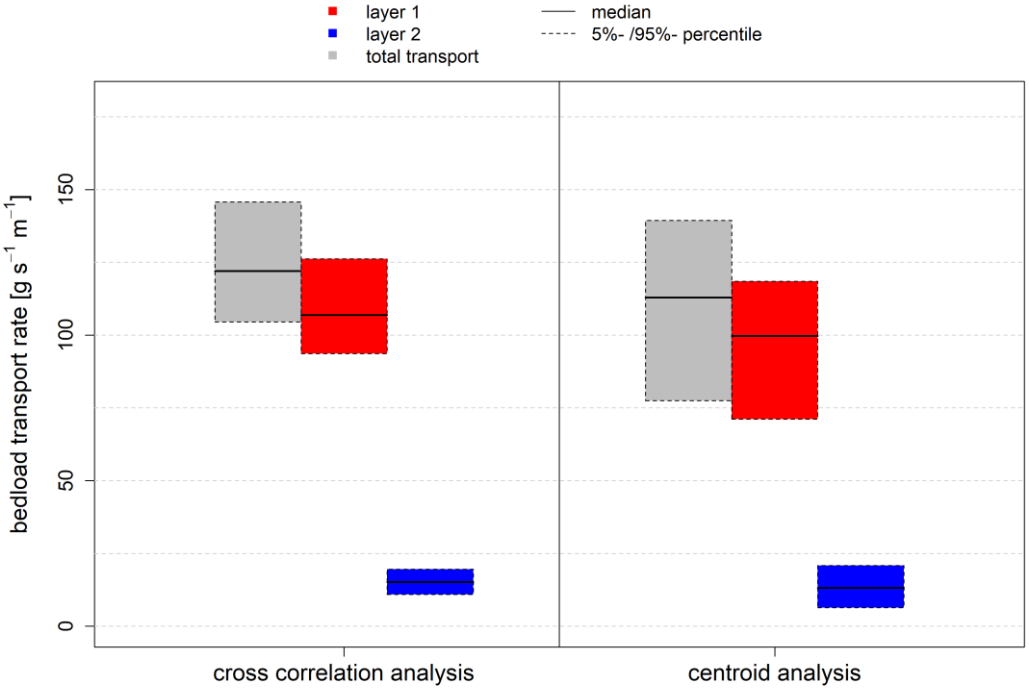

445

Figure 15: Comparison of bedload transport rates derived from cross-correlation and centroid analysis along the evaluated BEP.

5 Discussion

5.1 Sensitivity of the input parameters

450 The presented dunetracking tool requires several input parameters. An MCS approach was shown capable to quantify the influence of these parameters on the calculation of bedform geometries and bedload transport rates. To address the question which of the input parameters has the greatest influence, a sensitivity analysis was performed, in which only one input parameter was varied at a time while the others were kept constant. Table 4 shows the three chosen input parameter settings. For the parameters that were kept constant, a mean value was set based on the results from wavelet analysis (see Figure 8).

455

Table 4: Input parameter for sensitivity analyses

setting	window size layer 1 [m]	window size layer 2 [m]	zc-threshold [cm]
1	1 – 20	25	0.5
2	8	20 – 30	0.5

https://doi.org/10.5194/egusphere-2024-579
Preprint. Discussion started: 25 April 2024
© Author(s) 2024. CC BY 4.0 License.

3	8	25	0.5 – 5

5.1.1 Bedform geometries

Figure 16 shows the potential influence of the parameters window sizes for layer 1 and 2 as well as zc-threshold on the resulting bedform geometries (T90, H_{total} $L_{1,2}$). The resulting bedform geometries were averaged over all BEPs, which has a stabilizing effect. Increasing the window size of layer 1 (setting 1) results in increasing bedform heights and lengths. The parameter is especially sensitive during the first iterations. When exceeding a value of about five meters, increasing convergence can be observed for both bedform heights and lengths. Within the selected range of window sizes based on Bedforms-ATM (grey area), only a very low variability can be observed. Overall, with respect to bedform height the T90-parameter behaves less sensitive than the H_{total}-parameter.

Window size of layer 2 (setting 2) has almost no influence on the T90-parameter. With respect to the H_{total}-parameter, a very slight increase (2 cm) can be observed with increasing window size. Bedform length (in this case only layer 2 is affected), again, exhibits more sensitivity. Here, no convergence can be observed. Nevertheless, variability is much smaller compared to setting 1.

The influence of the zc-threshold (setting 3) is also much smaller than that of the window size of layer 1. Bedform heights exhibit less sensitivity than bedform lengths, for which no convergence occurs. By increasing the zc-threshold, local minima are filtered out successively (see Sect. 2). Thereby, several individual bedforms are summarized, resulting in a smaller number of longer bedforms. This is why it is important to consider the expected bedform dimensions, in order not to obtain implausible results.

https://doi.org/10.5194/egusphere-2024-579
Preprint. Discussion started: 25 April 2024
© Author(s) 2024. CC BY 4.0 License.

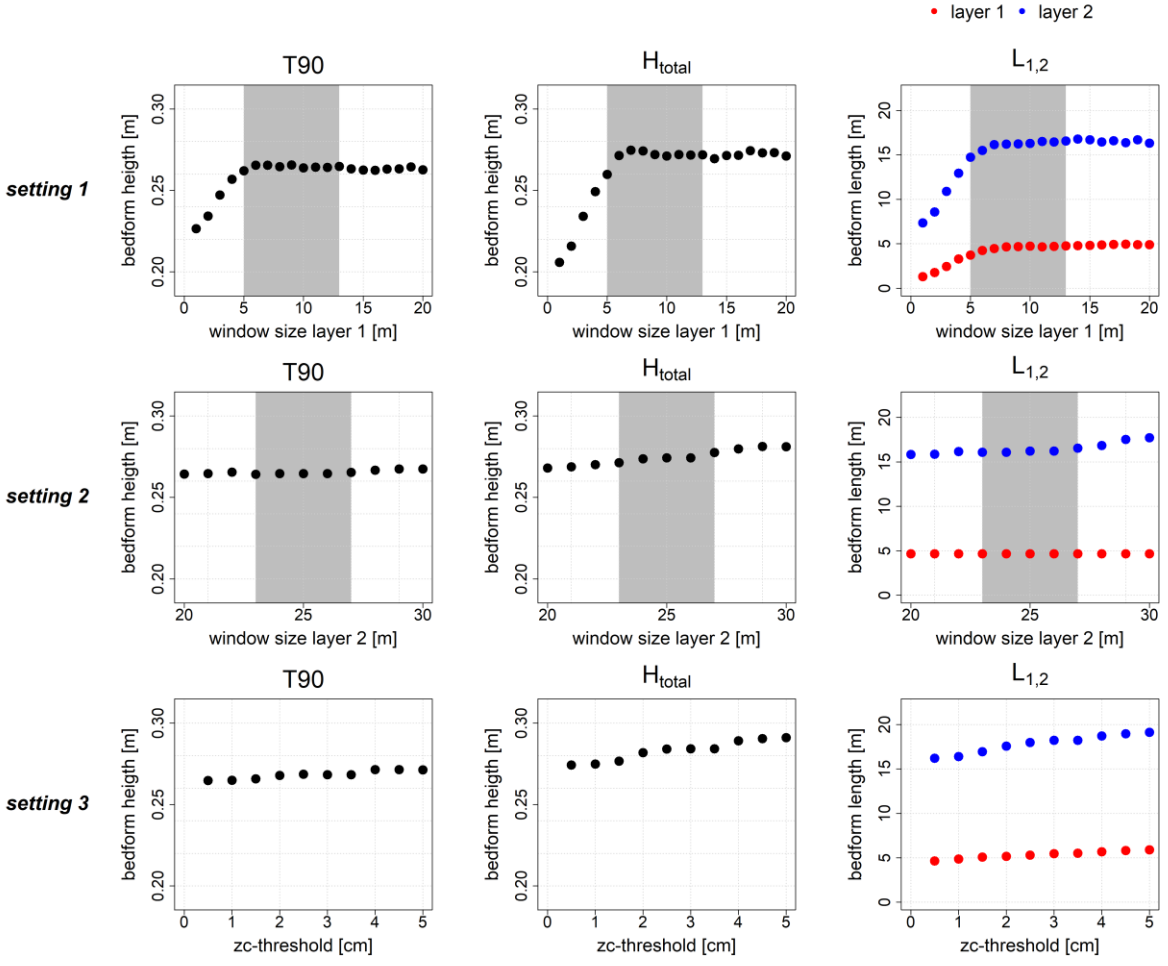

Figure 16: Influence of variation in the input parameters on derived bedform geometries (grey area corresponds to the selected value range based on Bedforms-ATM).

Changing window size of layer 1 has the strongest impact on resulting bedform geometries. Concerning bedform height, the T90-parameter appears to be more robust towards varying input parameter settings compared to the H_{total}-parameter. This can be explained by the fact that every point of the BEP is always included in the calculation of the T90-parameter and it is therefore independent of the number of detected bedforms in a subsection. Overall, bedform lengths appear to be much more sensitive and include a higher degree of uncertainty. The delineation of two adjacent bedforms is not always obvious and several different solutions might be conceivable. Even a manual delineation is a highly subjective process and could lead to different solutions for different investigators. For many cases a convergence pattern can be observed, that starts at the lower margin of window sizes based on the results from Bedforms-ATM (grey shaded area in Fig. 15). Window sizes smaller than the lower margin, lead to diverging results, which confirms the need for Bedforms-ATM as an orientation.

https://doi.org/10.5194/egusphere-2024-579
Preprint. Discussion started: 25 April 2024
© Author(s) 2024. CC BY 4.0 License.

These findings should be taken into account when analyzing bedform geometries, such as studies on the relationship between bedform height and length (e.g. Flemming 2000; Lefebvre et al. 2022). Individual bedform attributes are often displayed in scatterplots. According to the findings of this study, an uncertainty range would have to be specified for each data point in a scatterplot, based on different input parameter settings in the evaluation procedure.

5.1.2 Bedform migration & bedload transport

Figure 17 shows the results of the sensitivity analysis for the calculation of bedform migration and bedload transport rates based on the cross-correlation analysis (method 1). For this purpose, the resulting parameters were averaged over different measurement intervals. Based on the findings presented in Sect. 4.3, only measurement intervals shorter than two hours were considered for layer 1 whereas only measurement intervals longer 19 hours (measurements carried out on different days) were considered for layer 2.

Increasing window sizes for layer 1 lead to decreasing bedform migration rates that converge to a value of about 2 m s^{-1} for window sizes > 5m (Fig. 16). For smaller window sizes smaller bedforms are derived from the BEPs, which are migrating with higher rates. At the same time, bedload transport rates for layer 1 increase with increasing window size as bedform area increases, which overweighs the influence of decreasing migration rates. Bedform area for layer 2, however, decreases with increasing bedform area for layer 1 due to a different delineation of the total geometry. As a result, bedload transport rates for layer 2 decrease as well. Correlation coefficients increase with increasing window size for layer 1. This is because small bedforms resulting from small window sizes can only be traced accurately for very short measurement intervals. So, averaged correlation coefficients are lower for smaller window sizes. Layer 2 is only slightly affected. Overall, highest variability can be found outside the chosen range of window sizes for layer 1 based on Bedforms-ATM.

Varying window sizes for layer 2 do not have any influence on cross-correlation analysis. This is because the baselines of layer 2 are not included in the analysis (see Sect. 2). Only the changing (increasing) bedform areas result in a slight increase in bedload transport rates for layer 2.

Concerning the behavior of the zc-threshold, similar effects can be observed as for window size 1 at setting 1, however, they turn out to be significantly less sensitive. Basically, low values lead to a derivation of smaller bedforms with higher migration rates. Very high values on the other hand lead to the derivation of larger bedforms and to a different delineation of the total geometry. Correlation coefficients stay rather constant over all iterations.

https://doi.org/10.5194/egusphere-2024-579
Preprint. Discussion started: 25 April 2024
© Author(s) 2024. CC BY 4.0 License.

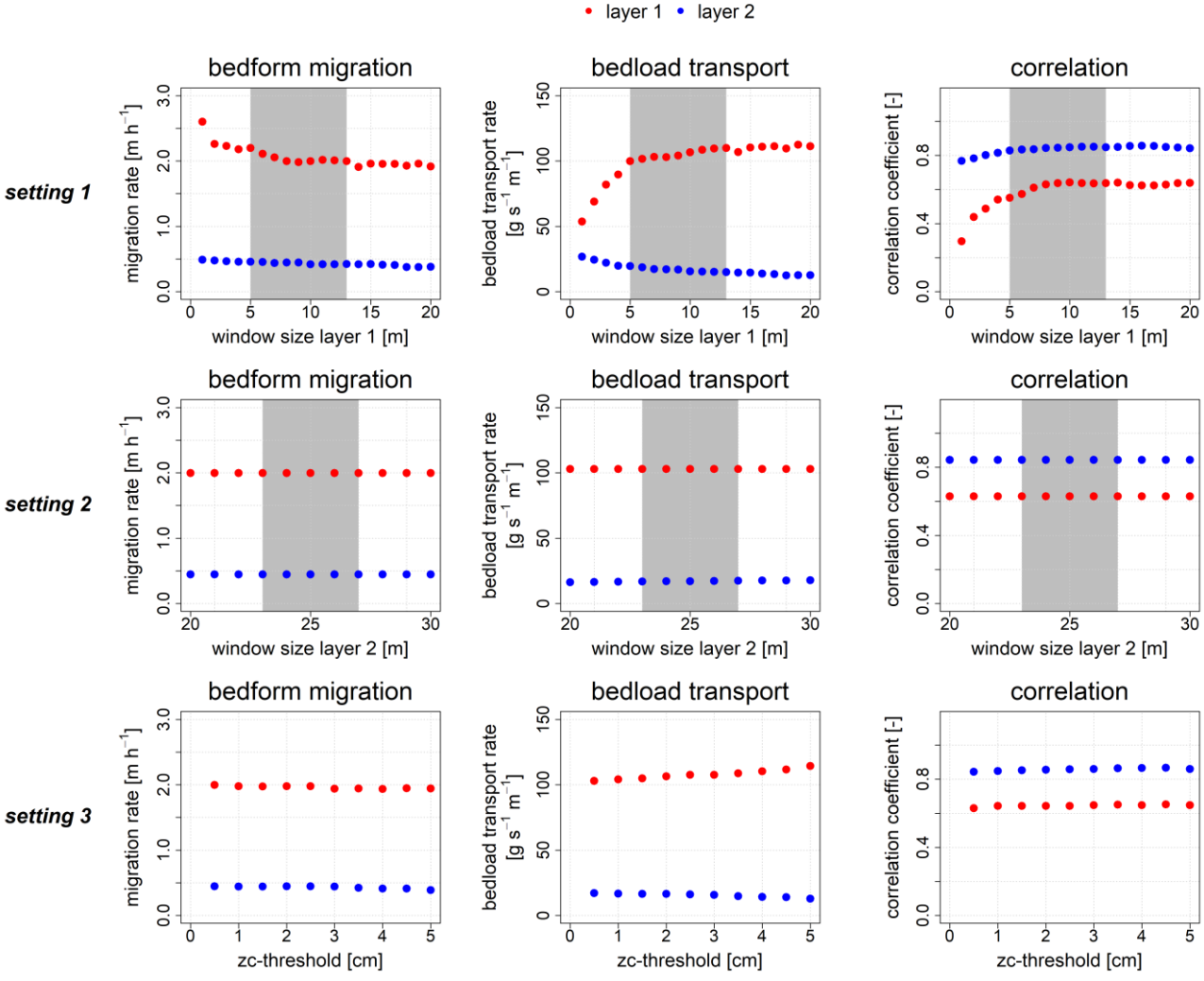

Figure 17: Sensitivity analysis of the input parameters of the cross-correlation analysis (grey area corresponds to the selected value range based on Bedforms-ATM).

Figure 18 shows the influence of input parameter settings on centroid analysis (method 2). As explained in the previous sections the method is only suitable for small bedforms and short measurement intervals. This is why only bedforms of layer 1 and only those measurement pairs with intervals shorter than two hours are considered here (see Sect. 4).

At setting 1, migration rates initially increase with increasing window size. A maximum is reached at a value of 3 m. A further increase in window size leads to decreasing migration rates with a tendency to convergence to a value of 1.5 m s^{-1}. Bedload transport rates first increase and then tend towards a value of 100 g s^{-1} m^{-1}. Very small bedforms can only be traced accurately at very short measurement intervals, so that a rapid increase in the number of detected bedforms can be observed with

https://doi.org/10.5194/egusphere-2024-579
Preprint. Discussion started: 25 April 2024
© Author(s) 2024. CC BY 4.0 License.

increasing window size. After reaching a maximum at a value of 10 m the number of traceable bedforms decreases again. An increasing window size leads to increasing bedform areas and thus to a decreasing number of bedforms. Again, for all parameters highest variations are found outside the chosen range of window sizes.

Varying the setting of the zc-threshold again has much less impact on the results. No systematic effect on centroid analysis can be observed.

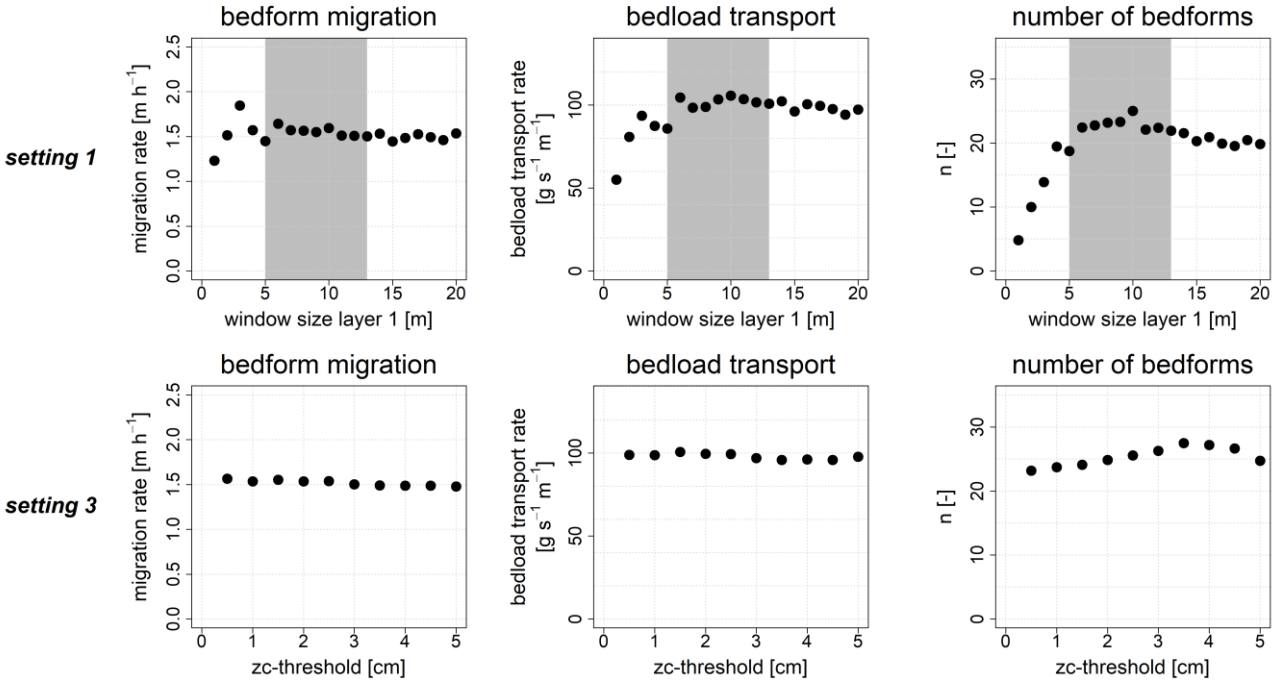

Figure 18: Influence of variation in the input parameters on centroid analysis (grey area corresponds to the selected value range based on Bedforms-ATM).

As for bedform geometry, it can also be observed for bedform migration and bedload transport that setting 1 has the greatest influence on the resulting parameters. This is true for both methods. Again, outside the chosen range of window sizes based on the results from Bedforms-ATM, increasing divergence can be seen.

5.2 Influence of measurement interval and evaluation methods on determination of bedform dynamics

The results for bedform migration and bedload transport rates show that the time interval between two consecutive measurements turns out to have a significant influence on the determination of bedform dynamics (see Sect. 4.3). There is a high variability in bedform migration rates depending on bedform dimensions. This is particularly evident, when looking at the individual migration rates that emerged from centroid analysis. The measurement interval determines the highest possible traceable migration rate and thus, at the same time, the minimum bedform dimensions that can be considered (since it is assumed that migration rates increase with decreasing bedform dimensions). The shorter the measurement interval, the smaller

https://doi.org/10.5194/egusphere-2024-579
Preprint. Discussion started: 25 April 2024
© Author(s) 2024. CC BY 4.0 License.

the bedforms that can be tracked accurately. An increase in measurement interval leads to an increasing loss of information and eventually to a potential underestimation of bedload transport rates, since the faster migrating smaller bedforms are no longer identified. These were only traceable for shortly consecutive measurements with time intervals of a few hours due to deformation. On the other hand, in order to track the underlying larger bedforms, longer measurement intervals appeared to be more suitable as they are subject to significantly lower scattering. However, it was shown that the migration of small bedforms accounted for about 90 % of the total bedload transport. This was found by applying both, cross-correlation and centroid analysis, which underlines the need for repeat measurements in high temporal resolution, in order to achieve an accurate mapping of all transport processes involved. It may be helpful to perform preliminary measurements to get a first impression about prevailing bedform dimensions and migration rates and to select a suitable interval based on this.

In this study, two methods for determining bedform dynamics were used. The newly introduced centroid analysis appeared to be subject to greater uncertainties with a range of uncertainty of about 50 % concerning total bedload transport rates, whereas for cross-correlation analysis a range of about 30 % could be identified. However, median values were found in the same order of magnitude for both methods. Nevertheless, the new approach allows a deeper look at the behavior of individual bedforms – in relation to their geometric attributes – as well as at the longitudinal variability of transport. From this, new insights can be gained especially concerning the behavior of rapidly migrating smaller bedforms, which can end up contributing the largest part to the total bedload transport.

For estimating bedload transport an approach based on Ten Brinke (1999) was used that includes grain density and porosity. For defining these parameters assumptions were made. So far, the estimated uncertainties of the results are only due the variation of the input parameters in the zerocrossing procedure and the different measurement intervals. The MCS could be extended to consider the uncertainty in setting a value for porosity and grain density. Since both parameters are linearly related to bedload transport, a variation of e.g. 10% will also result in a change of 10% concerning bedload transport rates. So, this uncertainty would have to be added to the results.

A more detailed look at the performance of different bedload transport measurement techniques and – among other aspects - at possible factors influencing the dunetracking method were the subject of the so-called LILAR-campaign (BfG, 2023). The campaign was carried out in november 2021 as cooperation of German and Dutch authorities. One of the objectives was to compile, compare and evaluate different methods for measuring sediment transport.

Conclusions

Dunetracking tools are sensitive to the influence of several input parameters. No theoretically sound criteria are available for the setting of input parameters with specific values. So, this decision depends on the subjective assessment of the investigator. By combining two existing tools and by adding a Monte Carlo Simulation, a new dunetracking tool was developed which enables the automated processing of large datasets as well as the quantification of procedure specific uncertainties in the

https://doi.org/10.5194/egusphere-2024-579
Preprint. Discussion started: 25 April 2024
© Author(s) 2024. CC BY 4.0 License.

calculation of bedform parameters. The MCS allows the implementation of robust estimates and reveals the possible range of solutions based on different input parameter settings. In this study the following key findings were identified.

- Bedform parameters react with different sensitivity to varying input parameter settings. With respect to bedform geometries, lengths are more affected than heights. Here, a scattering of up to 50% of the mean bedform length is reached (in individual BEPs). Concerning bedform heights, the introduced T90-parameter has proven to be more robust compared to the H_{total}-parameter, which is based on averaging individual bedform heights. Uncertainties regarding bedform geometries are propagated in the determination of bedform migration and bedload transport rates.
- Uncertainties for bedload transport rates were found in the order of 30% (by using cross correlation analysis) to 50% (by using centroid analysis). By applying both methods it could be shown that the migration of secondary bedforms accounted for about 90 % of the total bedload transport.
- Regarding bedform dynamics there also is an uncertainty due to different time intervals between two consecutive measurements. Rapidly migrating secondary bedforms were only traceable for shortly consecutive measurements with time intervals of less than two hours. This underlines the need for measurements in high temporal resolution.
- With regard to the question of which input parameter has the greatest influence on the resulting bedform parameters, window size for layer 1 was identified as the most sensitive. Especially for very small values, an increase in window size has a significant impact on bedform geometries as well as on bedform migration and bedload transport rates.
- The most stable results were found inside the range of values provided by the wavelet analysis (Bedforms-ATM) in the first step of the workflow. This underlines the importance of performing the wavelet analysis to narrow the range of values entering the MCS. It was shown that values below the specified range strongly influence the results and lead to divergence.
- Overall, the MCS identifies a range of uncertainty, which is an essential aspect that should be included as additional information in field studies characterizing prevailing bedform conditions derived from measurement data.

Perspectively, the developed workflow can be extended by further aspects in order to obtain an even more comprehensive determination of process-specific uncertainties in dunetracking methods.

Appendices

Appendix A

Table A1: 45 evaluated measurement pairs obtained from detail measurements

no.	date 1	time 1 (MET)	date 2	time 2 (MET)	Δt [h]

https://doi.org/10.5194/egusphere-2024-579
Preprint. Discussion started: 25 April 2024
© Author(s) 2024. CC BY 4.0 License.

1	18 February 2020	10:29	18 February 2020	10:41	0.2
2	18 February 2020	10:41	18 February 2020	11:05	0.4
3	18 February 2020	10:29	18 February 2020	11:05	0.6
4	18 February 2020	11:05	18 February 2020	11:57	0.9
F5	17 February 2020	11:17	17 February 2020	12:13	0.9
6	18 February 2020	10:41	18 February 2020	11:57	1.3
7	18 February 2020	10:29	18 February 2020	11:57	1.5
8	18 February 2020	11:57	18 February 2020	13:36	1.6
9	18 February 2020	8:46	18 February 2020	10:29	1.7
10	19 February 2020	9:24	19 February 2020	11:12	1.8
11	18 February 2020	8:46	18 February 2020	10:41	1.9
12	18 February 2020	8:46	18 February 2020	11:05	2.3
13	18 February 2020	11:05	18 February 2020	13:36	2.5
14	18 February 2020	10:41	18 February 2020	13:36	2.9
15	18 February 2020	10:29	18 February 2020	13:36	3.1
16	18 February 2020	8:46	18 February 2020	11:57	3.2
17	18 February 2020	8:46	18 February 2020	13:36	4.8
18	18 February 2020	13:36	19 February 2020	9:24	19.8
19	17 February 2020	12:13	18 February 2020	8:46	20.6
20	18 February 2020	11:57	19 February 2020	9:24	21.4
21	17 February 2020	11:17	18 February 2020	8:46	21.5
22	18 February 2020	13:36	19 February 2020	11:12	21.6
23	17 February 2020	12:13	18 February 2020	10:29	22.3
24	18 February 2020	11:05	19 February 2020	9:24	22.3
25	17 February 2020	12:13	18 February 2020	10:41	22.5
26	18 February 2020	10:41	19 February 2020	9:24	22.7
27	17 February 2020	12:13	18 February 2020	11:05	22.9
28	18 February 2020	10:29	19 February 2020	9:24	22.9
29	17 February 2020	11:17	18 February 2020	10:29	23.2
30	18 February 2020	11:57	19 February 2020	11:12	23.2
31	17 February 2020	11:17	18 February 2020	10:41	23.4

https://doi.org/10.5194/egusphere-2024-579
Preprint. Discussion started: 25 April 2024
© Author(s) 2024. CC BY 4.0 License.

32	17 February 2020	12:13	18 February 2020	11:57	23.7
33	17 February 2020	11:17	18 February 2020	11:05	23.8
34	18 February 2020	11:05	19 February 2020	11:12	24.1
35	18 February 2020	10:41	19 February 2020	11:12	24.5
36	18 February 2020	8:46	19 February 2020	9:24	24.6
37	17 February 2020	11:17	18 February 2020	11:57	24.7
38	18 February 2020	10:29	19 February 2020	11:12	24.7
39	17 February 2020	12:13	18 February 2020	13:36	25.4
40	17 February 2020	11:17	18 February 2020	13:36	26.3
41	18 February 2020	8:46	19 February 2020	11:12	26.4
42	17 February 2020	12:13	19 February 2020	9:24	45.2
43	17 February 2020	11:17	19 February 2020	9:24	46.1
44	17 February 2020	12:13	19 February 2020	11:12	47
45	17 February 2020	11:17	19 February 2020	11:12	47.9

Code & data availability

The introduced tool (code and test dataset) is accessible via: https://github.com/JRbfg/DTMCS

Author contribution

JR developed the code, performed all analyses and prepared the paper with the cooperation of AW. AW provided support regarding the technical discussion of the results as well as regarding the composition of the paper.

Competing interests

The contact author has declared that none of the authors has any competing interests.

Acknowledgements

The measurements to collect test dataset used in this paper were performed by the Federal Waterways and Shipping Administration (Wasserstraßen- und Schifffahrtsverwaltung des Bundes, WSV). The hydrographic processing and the

https://doi.org/10.5194/egusphere-2024-579
Preprint. Discussion started: 25 April 2024
© Author(s) 2024. CC BY 4.0 License.

provision of the individual BEPs were carried out by Felix Lorenz and Thomas Artz from the Federal Institute of Hydrology (Department for Geodesy and Remote Sensing). We are grateful for the provision of the data.

Funding

Large parts of this work were part of the MAhyD project (morphodynamic analyses using hydroacoustic data, Morphodynamische Analysen mittels hydroakustischer Daten – Sohlstrukturen und Geschiebetransport). The MAhyD project was funded by the Federal Ministry for Digital and Transport (BMDV).

References

BfG (2011). Sedimentologisch-Morphologische Untersuchung des Niederrheins. BfG 1768, 32.

BfG (2023). Living Lab Rhine (LILAR): Comparison of Sediment Measurement Methods Between the Netherlands and Germany. BfG 2141,
Bundesanstalt für Gewässerkunde, Koblenz

Carling, P., Gölz, E., Orr, H., Radecki-Pawlik, A.. (2000). The morphodynamics of fluvial sand dunes in the River Rhine, near Mainz, Germany. I. Sedimentology and morphology. Sedimentology. 47. 227 - 252. 10.1046/j.1365-3091.2000.00290.x.

Claude, N., Rodrigues, S., Bustillo, V., Bréhéret, J., Macaire, J., Jugé, P.. (2012). Estimating bedload transport in a large sand–gravel bed river from direct sampling, dune tracking and empirical formulas. Geomorphology. 179. 40–57. 10.1016/j.geomorph.2012.07.030.

Flemming, B. (2000). The role of grain size, water depth and flow velocity as scaling factors controlling the size of subaqueous dunes. Marine Sandwave Dynamics, International Workshop, March 23-24 2000, University of Lille.

Frings, R.M., Gehres, N., de Jong, K., Beckhausen, C., Schüttrumpf, H. and Vollmer, S.. (2012). Rheno BT, User Manual, Institute of Hydraulic Engineering and Water Resources Management, RWTH Aachen University.

Gilja, G., Kuspilić, N., Brckan, B.. (2013). Computer algorithm for analysis of bedform geometry. Conference: 13th International Symposium on Water Management and Hydraulic Engineering

Gutierrez, R. R., Abad, J. D., Parsons, D. R., & Best, J. L.. (2013). Discrimination of bed form scales using robust spline filters and wavelet transforms: Methods and application to synthetic signals and bed forms of the Río Paraná, Argentina. Journal of Geophysical Research: Earth Surface, 118(3), 1400– 1418. https://doi.org/10.1002/jgrf.20102

Gutierrez, R.R., Mallma, J.A., Núñez-González, F., Link, O. and Abad, J.D.. (2018). Bedforms-ATM, an open source software to analyze the scale-based hierarchies and dimensionality of natural bed forms. SoftwareX, 7, pp.184-189.

Henning, M. (2013). Mehrdimensionale statistische Analyse räumlich und zeitlich hoch aufgelöster Oberflächen von Dünenfeldern.

https://doi.org/10.5194/egusphere-2024-579
Preprint. Discussion started: 25 April 2024
© Author(s) 2024. CC BY 4.0 License.

Kleinhans, M.. (2001). The key role of fluvial dunes in transport and deposition of sand–gravel mixtures, a preliminary note. Sedimentary Geology. 143. 7-13. 10.1016/S0037-0738(01)00109-9.

Kleinhans, M., Wilbers, A.W.E., Swaaf, A., Berg, J.. (2002). Sediment Supply-Limited Bedforms in Sand-Gravel Bed Rivers. Journal of Sedimentary Research. 72. 10.1306/030702720629.

Leary, K. & Buscombe, D.. (2020). Estimating sand bed load in rivers by tracking dunes: a comparison of methods based on bed elevation time series. Earth Surface Dynamics. 8. 161-172. 10.5194/esurf-8-161-2020.

Lefebvre, A. & Winter, C.. (2016). Predicting bed form roughness: the influence of lee side angle. Geo-Marine Letters. 36. 10.1007/s00367-016-0436-8.

Lefebvre, A., Herrling, G., Becker, M., Zorndt, A., Krämer, K. & Winter, C. (2022). Morphology of estuarine bedforms, Weser Estuary, Germany. Earth Surface Processes and Landforms, 47(1), 242–256. Available from: https://doi.org/10.1002/esp.5243

Lorenz, F., Artz, T., Brüggemann, T., Reich, J., Weiß, R., Winterscheid, A. (2021). Simulation-based Evaluation of Hydrographic Data Analysis for Dune Tracking on the River Rhine. PFG – Journal of Photogrammetry Remote Sensing and Geoinformation Science. 89. 1-10. 10.1007/s41064-021-00145-0.

McElroy, B., Mohrig, D.. (2009). Nature of deformation of sandy bed forms, J. Geophys. Res.-Earth, 114, F00A04, https://doi.org/10.1029/2008JF001220.

Nyander, A., Addison, P.S., McEwan, I., Pender, G.. (2003). Analysis of river bed surface roughnesses using 2D wavelet transform-based methods. The Arabian Journal for Science and Engineering, 28(1C):107-121.

Ogor, J. (2018). Design of algorithms for the automatic characterization of marine dune morphology and dynamics. Ocean, Atmosphere. ENSTA Bretagne - École nationale supérieure de techniques avancées Bretagne.

OpenStreetMap contributors. Planet dump retrieved from https://planet.openstreetmap.org (accessed on 23 August 2023).

Raja, J., Muralikrishnan, B., Fu, S.. (2002). Recent advances in separation of roughness, waviness and form. Precision Engineering, 26:222-235.

Simons, D. B., Richardson, E. V., Nordin, C. F.. (1965) Bedload equation for ripples and dunes, US Government Printing Office, Washington D.C., USA.

Ten Brinke, W.B.M., Wilbers, A.W.E., Wesseling, C. (1999): Dune growth, decay and migration rates during large-magnitude flood at sand and mixed sand-gravel bed in the Dutch Rhine river system. Special Publication of the International Association of Sedimentologists 28, 15-32.

Van der Mark, R., Blom, A.. (2007). A new and widely applicable tool for determining the geometric properties of bedforms. 10.13140/RG.2.2.17637.40161.

Van Rijn, L.C.. (1993). Principles of sediment transport in rivers, estuaries and coastal seas.

Van Rijn, L.C.. (2007). Unified View of Sediment Transport by Currents and Waves. I: Initiation of Motion, Bed Roughness, and Bed-Load Transport. Journal of Hydraulic Engineering. 133. 10.1061/(ASCE)0733-9429(2007)133:6(649).

Venditti, J.. (2013). 9.10 Bedforms in Sand-Bedded Rivers. 10.1016/B978-0-12-374739-6.00235-9.

https://doi.org/10.5194/egusphere-2024-579
Preprint. Discussion started: 25 April 2024
© Author(s) 2024. CC BY 4.0 License.

Wang, L., Yu, Q., Gao, S.. (2019). A combined method to calculate superimposed 2-D dune morphological parameters. Conference: Marine and River Dune Dynamics 2019 (MARID VI)

Wesseling, C., Wilbers, A. W. E.. (2000). Manual DT2D version 2.3: Software for dune-tracking in two dimensions. (In Dutch). Tech. rep., Faculteit der Ruimtelijke Wetenschappen, Universiteit Utrecht, Utrecht.

Zomer, J.Y., Naqshband, S., Hoitink, A.J.F.. (2021). Short communication: A new tool to define multiscale bedform characteristics from bed elevation data. 10.5194/esurf-2021-98.

Zomer, J.Y., Naqshband, S., Vermeulen, B., Hoitink, A.J.F.. (2021). Rapidly migrating secondary bedforms can persist on the lee of slowly migrating primary river dunes. Journal of Geophysical Research; Earth Surface, 126, e2020JF005918.